

# Fluvial Carbon Dynamics across the Land to Ocean Continuum of Great Tropical Rivers: the Amazon and Congo

Jeffrey Richey<sup>1</sup>, Robert Spencer<sup>2</sup>, Travis Drake<sup>3</sup>, and Nicholas Ward<sup>4</sup>

<sup>1</sup>University of Washington

<sup>2</sup>Florida State University

<sup>3</sup>ETH Zurich

<sup>4</sup>Pacific Northwest National Laboratory

November 23, 2022

## Abstract

Many rivers systems of the world are super-saturated in dissolved CO<sub>2</sub> (pCO<sub>2</sub>) relative to equilibrium with the atmosphere — why? Here we compare the coupled organic matter and pCO<sub>2</sub> dynamics of the world's two largest river systems, the Amazon and Congo, where data sets enable insights into the overall functioning of the respective basins. Discharge is the primary control on particulate (POC) and dissolved organic carbon (DOC) export in both the Amazon and Congo Rivers. Total suspended sediments (TSS) yield from the Amazon is twenty times greater per unit area than the Congo. However, despite low TSS concentrations, the Congo has a POC content approximately five times higher than the Amazon. The organic rich character of both watersheds is reflected in the DOC export, with the Amazon exporting ~ 11% and the Congo ~ 5% of the global land to ocean flux, based on measurements from the last discharge gauging stations. But care should be taken when describing estimates of TSS and carbon to the ocean. Processing and sequestration in tidal and coastal areas can significantly alter TSS and carbon delivery, and last discharge gauging stations are typically hundreds of kilometers from the sea. pCO<sub>2</sub> in the Amazon mainstem ranges from 1,000 to 10,000  $\mu$ atm, with floodplain lakes ranging from 20 to 20,000  $\mu$ atm. Concentrations in the Congo mainstem are lower, with maximum values of ~5,000  $\mu$ atm observed. The elevated level of pCO<sub>2</sub> even as far as the mouth of such major rivers as the Amazon and Congo, up to thousands of kilometers from CO<sub>2</sub>-rich small streams, poses a most interesting question — what set of processes maintains such high levels? The answer is presumably some combination of instream metabolism of organic matter of terrestrial and floodplain origin, and/or injection of very high pCO<sub>2</sub> water from local floodplains or tributaries.

## Hosted file

acknowledgments.docx available at <https://authorea.com/users/544696/articles/601796-fluvial-carbon-dynamics-across-the-land-to-ocean-continuum-of-great-tropical-rivers-the-amazon-and-congo>



AGU Books

## Fluvial Carbon Dynamics across the Land to Ocean Continuum of Great Tropical Rivers: the Amazon and Congo

Journal:	<i>AGU Books</i>
Manuscript ID	2020-May-CH-1259.R1
Wiley - Manuscript type:	Chapter
Date Submitted by the Author:	n/a
Complete List of Authors:	Richey, Jeffrey; University of Washington, School of Oceanography Spencer, Rob; Florida State University, Earth, Ocean and Atmospheric Sciences Drake, Travis; ETH Zürich, Environmental Systems Science Ward, Nicholas; University of Washington, School of Oceanography; Pacific Northwest National Laboratory Marine Sciences Laboratory
Primary Index Term:	428 - Carbon cycling (4806) < 400 - BIOGEOSCIENCES
Index Term 1:	1806 - Chemistry of fresh water < 1800 - HYDROLOGY
Index Term 2:	9305 - Africa < 9300 - GEOGRAPHIC LOCATION
Index Term 3:	9345 - Large bodies of water (e.g., lakes and inland seas) (0746) < 9300 - GEOGRAPHIC LOCATION
Index Term 4:	9360 - South America < 9300 - GEOGRAPHIC LOCATION
Keywords:	metabolism, rivers, Congo, Amazon, organics, pCO <sub>2</sub>
Abstract:	<p>Many rivers systems of the world are super-saturated in dissolved CO<sub>2</sub> (pCO<sub>2</sub>) relative to equilibrium with the atmosphere — why? Here we compare the coupled organic matter and pCO<sub>2</sub> dynamics of the world's two largest river systems, the Amazon and Congo, where data sets enable insights into the overall functioning of the respective basins. Discharge is the primary control on particulate (POC) and dissolved organic carbon (DOC) export in both the Amazon and Congo Rivers. Total suspended sediments (TSS) yield from the Amazon is twenty times greater per unit area than the Congo. However, despite low TSS concentrations, the Congo has a POC content approximately five times higher than the Amazon. The organic rich character of both watersheds is reflected in the DOC export, with the Amazon exporting ~ 11% and the Congo ~ 5% of the global land to ocean flux, based on measurements from the last discharge gauging stations. But care should be taken when describing estimates of TSS and carbon to the ocean. Processing and sequestration in tidal and coastal areas can significantly alter TSS and carbon delivery, and last discharge gauging stations are typically hundreds of kilometers from the sea. pCO<sub>2</sub> in the Amazon mainstem ranges from 1,000 to 10,000 μatm, with floodplain lakes ranging from 20 to 20,000 μatm. Concentrations in the Congo mainstem</p>

	<p>are lower, with maximum values of <math>\sim 5,000 \mu\text{atm}</math> observed. The elevated level of <math>\text{pCO}_2</math> even as far as the mouth of such major rivers as the Amazon and Congo, up to thousands of kilometers from <math>\text{CO}_2</math>-rich small streams, poses a most interesting question — what set of processes maintains such high levels? The answer is presumably some combination of instream metabolism of organic matter of terrestrial and floodplain origin, and/or injection of very high <math>\text{pCO}_2</math> water from local floodplains or tributaries.</p>

SCHOLARONE™  
Manuscripts

## 1 **1. Introduction**

2 The Amazon and the Congo combined account for ~25% of global river discharge to the oceans.  
3 Understanding the flow of pCO<sub>2</sub> and organic matter (OM) in these humid tropical basins is an  
4 important part of understanding the role of fluvial systems in the global carbon cycle. The classic  
5 perspective for the role of rivers is that they simply export terrestrially-derived OM to the world's  
6 oceans, where long-term preservation occurs largely along continental margins. However, rivers  
7 are now conceptualized as an 'active pipe' (Cole et al., 2007) with inputs sequestered in sediments,  
8 evaded to the atmosphere or exported to the ocean (Cole et al., 2007; Ward et al., 2017). This  
9 paradigm shift results from knowledge that rivers and other inland waters outgas immense  
10 quantities of CO<sub>2</sub> to the atmosphere. While Wissmar et al. (1981) were the first to call attention to  
11 this for the Amazon River, it took years for the consequences to be more fully understood. Richey  
12 et al. (2002) estimated that the Amazon River Basin emits roughly 0.5 Pg C yr<sup>-1</sup> from aquatic  
13 systems to the atmosphere as CO<sub>2</sub> and scaled these rates to a global estimate of ~1 Pg C yr<sup>-1</sup>. To  
14 put the Amazon River value in context, it is roughly comparable to net ecosystem exchanges in  
15 non-inundated upland forests derived from eddy covariance measurements (Malhi and Grace,  
16 2000). New global estimates of the surface area of aquatic systems (Allen and Pavelsky, 2018),  
17 models for gas transfer velocities, and observations of aquatic CO<sub>2</sub> concentrations have resulted  
18 in a 2-3 fold increase in global estimates of inland water CO<sub>2</sub> emissions (Raymond et al., 2013;  
19 Drake et al., 2017; Sawakuchi et al., 2017).

20 These observations pose three primary questions – (1) what are the geographic distributions  
21 and magnitude of aquatic CO<sub>2</sub> outgassing, (2) what are the biological and physical processes that  
22 ultimately drive the outgassing, and (3) how should the cycles producing such fluxes be  
23 incorporated into the overall carbon cycle of a large river basin, among water, land, and

24 atmosphere? Addressing these questions is very complicated. To assess the overall outgassing  
25 dynamics for a river basin requires examining much more than just the main channel. Melack  
26 (2016) identifies small streams, medium tributaries, river mainstem, lakes, river-adjacent  
27 floodplains and other wetlands as having their own respective dynamics. Further, each of these  
28 environments change dramatically over the course of the annual hydrograph and from year to year.  
29 River impoundments can also substantially modify the hydrological and biogeochemical behavior  
30 of aquatic ecosystems (St. Louis et al., 2000; Tranvik et al., 2009; Araújo et al., 2019).

31 While the Amazon River has been relatively well-studied, there is much less information for  
32 the Congo River. Alsdorf et al. (2016) summarized what was known at the time on the fluxes of  
33 total suspended sediments (TSS), particulate and dissolved organic carbon (POC, DOC), and  
34 dissolved greenhouse gases ( $\text{CO}_2$  and  $\text{CH}_4$ ) in the Congo River. They posed the hypothesis that  
35 “the annual-average amount of  $\text{CO}_2$  and  $\text{CH}_4$  evasion from all Congo Basin waters is more than  
36  $480 \text{ Tg C yr}^{-1}$ , i.e., more than a value comparable to that of the Amazon per unit area.”

37 The emerging data sets for the Congo River, joint with Amazon River data, enable us to begin  
38 to think more generally about the overall functioning of the world’s two largest river basins. Our  
39 primary intent here is to examine in more detail the relative magnitudes and composition of  $\text{pCO}_2$   
40 and OM in the Congo River relative to the Amazon River, with an emphasis on the main channel  
41 of each river. Studies of large river systems typically stop at the last discharge gauging station,  
42 which may be many kilometers upstream from the ocean. Here we will extend the analysis to the  
43 full complement of the river to ocean continuum, recognizing that a river plume extending out into  
44 the ocean is still an integral part of the river system.

45 To keep track of all components of the fluvial carbon cycle for a river reach, it is useful to track  
46 the processes controlling  $\text{pCO}_2$  and OM through the lens of Net Ecosystem Exchange (NEE, *sensu*

47 Lovett et al., 2006; Cole et al., 2000; Butman and Raymond, 2011). NEE, the change in  $p\text{CO}_2$  over  
 48 time and distance, can be expressed mathematically (following Devol et al., 1995) as:

$$49 \quad d(p\text{CO}_2)/dt = \text{NEE} = \text{Net advection } [I + T \pm F - O] + \text{Net Metabolism } [R - \text{GPP}] - G + \text{NB}$$

50 where I is upstream input (discharge x concentration), T is tributary inputs, F is floodplain  
 51 exchange, O is downstream output, R is respiration (as a function of OM substrates), GPP is gross  
 52 primary production, G is gas exchange, and NB is non-biological reactions (e.g., photo-oxidation).

53 While the existing data are far from complete enough to compute NEE for each river, it does  
 54 provide a useful organizing framework.

55 While we focus our discussion of inland water greenhouse gases specifically on  $\text{CO}_2$ , methane  
 56 ( $\text{CH}_4$ ) is certainly also important. Information on methane cycling in the Amazon River and its  
 57 wetlands have been presented in studies such as Sawakuchi et al. (2014, 2016), Melack et al.  
 58 (2004), Pangala et al. (2017), Barbosa et al. (2009, 2020), with fewer studies available for the  
 59 Congo River (e.g., Borges et al., 2015; 2019).

## 61 2. The Regions

62 The Amazon and Congo Rivers (Figure 1) are the two largest rivers on Earth in terms of their  
 63 discharge ( $\sim 6,590 \text{ km}^3 \text{ yr}^{-1}$  at the last discharge gauging station and  $\sim 7,600 \text{ km}^3 \text{ yr}^{-1}$  to the sea, and  
 64  $\sim 1,325 \text{ km}^3 \text{ yr}^{-1}$ , respectively), and their watershed areas ( $6.1 \text{ Mkm}^2$  and  $3.7 \text{ Mkm}^2$ , respectively).  
 65 These two massive rivers drain large areas of predominantly tropical rainforest and savannah. The  
 66 Congo River Basin contains some of the most pristine areas of rainforest remaining on Earth, as



67 well as fewer dams in comparison to the Amazon River Basin (Laporte et al., 2007; Duveiller et  
68 al., 2008; Winemiller et al., 2016). A major feature of the central Congo is the Cuvette Centrale, a  
69 shallow depression overlain by swamp forest, with extensive peat deposits (Darghie et al., 2017).  
70 The mainstem of the Amazon River is bordered by an extensive floodplain (or várzea), with  
71 seasonally flooded savannas across the basin. There are marked distinctions in topography (with  
72 the Amazon receiving significant TSS inputs from the Andes), and land cover (with more abundant  
73 savannah-mosaic and perennially flooded wetlands in the Congo Basin compared to the Amazon,  
74 which has less savannah and the strongly seasonal floodplain).

75 Óbidos has been the traditional terminal measuring point for the Amazon River. Between  
76 Óbidos and the ocean, an additional ~20% discharge is added by lowland tributaries (roughly  
77 double the volume of the Mississippi River). The lower part of the reach is split around the island  
78 of Marajó, where tides of ~3 m (detectable nearly 600km upstream) produce semi-diurnal fluxes  
79 to and from floodplains and channels, resulting in complete flow reversal (though no salinity  
80 intrusion).

81 Although these two immense rivers drain tropical watersheds, there are clear differences in  
82 annual precipitation between them resulting in higher specific discharge (discharge per unit  
83 upstream area) in the Amazon River. Fluctuations in the Intertropical Convergence Zone induce  
84 wet and dry seasons in alternating seasons in the northern and southern sides of the Amazon Basin,  
85 resulting in a single peak of maximum flow at Óbidos in May-July, with a minimum in October-  
86 November (Richey et al. 1989, multiple sources). Precipitation ranges from less than 2,000 mm/yr  
87 in the extreme northeastern and southern parts of the Basin, to more than 3,500 mm/yr in the  
88 northwest lowlands and increases to 7,000 mm/yr on the east side of the Andes. South of the

89 equator there is a distinct dry period from June to August, whereas north of the equator the dry  
90 period lasts from January to March.

91 The Congo River exhibits less seasonal and interannual variability in river discharge than the  
92 Amazon River (Coynel et al., 2005; Richey et al., 1989; Spencer et al., 2012). Due to its position  
93 straddling the Equator, the Congo River near its mouth at Kinshasa-Brazzaville exhibits a bimodal  
94 hydrologic cycle with maximum flows in November-December and May, and minimum flows in  
95 August and March. The largest discharge maximum in November-December is due to increased  
96 discharge from the northern tributaries and is complemented by southern tributaries where water  
97 discharge begins to increase around the same time. The smaller May discharge maximum is driven  
98 by an increase from the southern part of the Basin by savannah draining tributaries (Coynel et al.,  
99 2005; Spencer et al., 2012). Given an estimated total global discharge to the ocean of  $36,000 \text{ km}^3$   
100  $\text{yr}^{-1}$ , the Amazon and the Congo Rivers are responsible for  $\sim 21\%$  and  $3.5\%$  of freshwater discharge  
101 to the world's oceans, respectively.

102

### 103 **3. Advective Fluxes**

#### 104 **3.1. $\text{pCO}_2$ Distributions in the Mainstem, Tributaries, and Floodplains**

105 Borges et al. (2015; 2019) report on a series of ten field expeditions between 2010 and 2015 in  
106 the Congo River. Transects in the lowland reaches of the river network in the eastern and central  
107 part of the Basin, predominantly between Kisangani and Kinshasa were conducted at high water  
108 (HW, December 2013) and at falling water (FW, June 2014). The  $\text{pCO}_2$  values in the mainstem  
109 increased from upstream to downstream, with typically elevated tributary values.  $\text{pCO}_2$  ranged  
110 from 2,400 (HW) and 1,700 (FW)  $\mu\text{atm}$  in Kisangani to 5,350 (HW) and 2,900 (FW)  $\mu\text{atm}$  in  
111 Kinshasa, with an average in tributaries of  $8,300 \pm 4,100$  (HW) and  $8,050 \pm 5,300$  (FW)  $\mu\text{atm}$ .

112 pCO<sub>2</sub> in tributaries was in general higher than in the mainstem with a few exceptions, namely in  
113 rivers close to Kinshasa (1,600 to 1,900 HW and 1,100 to 2,500 FW μatm), due to degassing at  
114 waterfalls upstream of the sampling stations. The highest pCO<sub>2</sub> values (up to 16,950 μatm) were  
115 observed in streams draining the Cuvette Central.

116 There are several studies of the longitudinal distribution of pCO<sub>2</sub> in the Amazon River. The  
117 first recognition that pCO<sub>2</sub> was supersaturated was by Wissmar et al. (1981), in a transect of the  
118 *R/V Alpha Helix*, from upstream of the Napo River (Peru) to Óbidos, at high water in May 1977.  
119 They reported increasing pCO<sub>2</sub> values from upstream to downstream of 4,900 to 6,900 μatm, with  
120 a range of concentrations in tributaries and lakes, from 2,500 to 15,000 μatm. They hypothesized  
121 that the respiratory input of CO<sub>2</sub> was balanced by outgassing but commented that this needed  
122 further examination.

123 The next systematic evaluation of pCO<sub>2</sub> (and related carbon species) was conducted by the  
124 *CAMREX* program, resulting in eight synoptic "snapshots" of the spatial and temporal variability  
125 of the chemical species measured, from Santo Antônio do Ica to Óbidos (Richey et al., 1990). The  
126 mainstem was supersaturated in CO<sub>2</sub> with respect to the atmosphere by 10-20 times, with an overall  
127 mean of 3,800 μatm. In contrast to dissolved inorganic carbon (DIC) concentrations, pCO<sub>2</sub> did not  
128 change downstream at rising water (mean 3,000 μatm) and increased downstream at falling water  
129 from 3,200 to 5,300 μatm; downstream, increases in pCO<sub>2</sub> were accompanied by decreases in pH.  
130 At rising water, the tributaries were either comparable in pCO<sub>2</sub> to the mainstem (Madeira, Negro,  
131 Japurá Rivers), up to 5,900 μatm more enriched (Iça, Juruá, and Purus Rivers), or from 5,900 to  
132 14,800 μatm more enriched (Jutaí River). At falling water, the maxima for the Jutaí and Purús  
133 rivers were comparable to rising water, while the Iça, Juruá, and Japura rivers increased by 3,000-  
134 4,400 μatm. The Negro River increased slightly and the Madeira River decreased slightly.

135      Abril et al. (2014) conducted a series of transects along an 800 km section of the Central  
136 Amazon, between 2007-2011, reporting that values in the mainstem were consistent with the  
137 previous reports of 1,000 to 10,000  $\mu\text{atm}$ , with floodplain lakes ranging from 20 to 20,000  $\mu\text{atm}$ .  
138 Borges et al. (2015) conducted a series of five cruises along the Amazon River mainstem and  
139 mouths of tributaries between 2007 and 2010. Results were presented as aggregated bins,  
140 representing mainstem, tributaries >100 m and tributaries <100 m in width. With this lumped  
141 binning, it was not possible to see spatial or seasonal trends. The  $\text{pCO}_2$  values were consistent with  
142 the previous measurements, averaging 4,500  $\mu\text{atm}$  in the mainstem, with values to 16,900 pm in  
143 streams <100 m. These values are higher than the Congo mainstem, which was attributed to higher  
144 wetland coverage. Amaral et al (2019) reported on  $\text{pCO}_2$  at multiple environments across the  
145 Negro River and Amazon during different periods of the fluvial hydrological cycle, with values  
146 that ranged from 307 to 7,527  $\mu\text{atm}$ .

147      Sawakuchi et al. (2017) measured  $\text{pCO}_2$  and outgassing from Óbidos to the lower river near the  
148 region of Macapá, with extrapolations to the ocean, from 2014 to 2016, at low, rising, high, and  
149 falling water.  $\text{pCO}_2$  and outgassing were measured directly. Concentrations decreased from Óbidos  
150 towards Macapá, as the channels widened, and wind fetch increased, and increased from low water  
151 to high water. The average  $\text{pCO}_2$  including all seasons and sites measured in the lower Amazon  
152 River and its tributaries was  $2,914 \pm 1,768 \mu\text{atm}$ . The mainstem (averages of Óbidos, Almeirim,  
153 and Macapá) averaged  $3,218 \pm 1,656 \mu\text{atm}$ . The tributaries (Rios Xingu and Tapajós), had  
154 significantly lower  $\text{pCO}_2$  compared to the mainstem stations with values of  $1,322 \pm 1,545 \mu\text{atm}$ .  
155 Concentrations decreased from Óbidos to Macapá and decreased from 5,500  $\mu\text{atm}$  at high water  
156 to 1,800  $\mu\text{atm}$  at low water.

157

### 158 3.2. POC Fluxes

159 The Congo River has low TSS concentrations resulting in a flux to the Atlantic Ocean of ~ 30  
160 Tg yr<sup>-1</sup> (Coynel et al., 2005; Spencer et al., 2016), much lower than that estimated from the Amazon  
161 River (600 - 1,150 Tg yr<sup>-1</sup>; Meade et al., 1985; Richey et al., 1986; Filizola and Guyot, 2009).  
162 Therefore, even though the Congo Basin is ~ 40% smaller than the Amazon, the TSS yield (flux  
163 per unit area) from the Amazon is still proportionally twentyfold greater (~ 90-180 versus ~8.5 t  
164 km<sup>-2</sup> yr<sup>-1</sup> for the Amazon and Congo Rivers, respectively; Meade et al., 1985; Richey et al., 1986;  
165 Coynel et al., 2005; Filizola and Guyot, 2009). The relatively low TSS yield from the Congo is  
166 due to the comparative lack of mountainous headwaters, generally low relief topography, lack of  
167 highly erodible sedimentary rocks, limited fluctuation in seasonal discharge, and large lakes as  
168 well as the world's largest swamp forest in the central depression (Cuvette Centrale) that act as  
169 giant sediment traps (Laraque et al., 2009; Spencer et al., 2016).

170 However, despite low concentrations, Congo River TSS has been reported to have a high POC  
171 content (6.05 - 7.25 %), which is approximately five times higher than the Amazon River at its  
172 furthest downstream discharge gaging station, Óbidos (Hedges et al., 1986; Aufdenkampe et al.,  
173 2007; Spencer et al., 2012; 2016). Thus, the Congo River exports ~ 2 Tg C yr<sup>-1</sup> as POC to the  
174 Atlantic Ocean, resulting in a POC yield of ~ 0.6 g C m<sup>-2</sup> yr<sup>-1</sup> (Coynel et al., 2005; Spencer et al.,  
175 2016). Although this is lower than POC yield estimates from the Amazon (~ 0.9 - 1.0 g C m<sup>-2</sup> yr  
176 <sup>-1</sup>), it highlights the organic rich nature of Congo River TSS as the yield is comparable between the  
177 basins despite the POC flux being approximately three times greater from the Amazon (~ 6 Tg  
178 yr<sup>-1</sup>; Moreira-Turcq et al., 2003; Coynel et al., 2005).

179 Upstream processes set the seasonally varying template for what is propagated downstream.  
180 Care should be taken when describing estimates of TSS and POC “to the ocean” since inputs below

181 the last measuring station and processing and sequestration in tidal and coastal areas can  
182 significantly alter TSS and POC delivery. Estimates of TSS and POC fluxes for both rivers have  
183 typically been made upstream of any tidal influence (i.e., at Óbidos in the case of the Amazon  
184 River and at Kinshasa-Brazzaville for the Congo River). However, POC concentrations are about  
185 two times higher upstream at Óbidos compared to near the river mouth at Macapá (Ward et al.,  
186 2015), suggesting both that POC is lost in transit due to processes such as degradation and/or burial  
187 of suspended sediments along the tidal tributary network (Fricke et al., 2017). This highlights the  
188 need to study large rivers in their lower reaches, downstream of the head of tides, to accurately  
189 account for material fluxes to the ocean (and atmosphere).

190

### 191 **3.3. DOC Fluxes**

192 With respect to DOC fluxes, the Amazon River at Óbidos has been estimated to export ~ 22-27  
193 Tg C yr<sup>-1</sup> (Richey et al. 1990; Moreira-Turcq et al., 2003) which amounts to 11% of the global  
194 DOC flux from river mouths, or more accurately the last gauging stations, to the ocean. If  
195 downstream major lowland tributaries are also included (e.g., the Tapajós and Xingu rivers; 1.5  
196 and 1.0 Tg C yr<sup>-1</sup> respectively), the total flux of the Amazon to the Atlantic is ~ 29.4 Tg C yr<sup>-1</sup>  
197 (Moreira-Turcq et al., 2003; Coynel et al., 2005). Indeed, measurements made near the mouth of  
198 the Amazon River at Macapá show an increase in DOC concentrations of 1.2 times compared to  
199 concentrations at Óbidos as a result of the tributary inputs and floodplain interactions along the  
200 tidally-influenced reaches of the river (Ward et al., 2015; Seidel et al., 2016).

201 The Congo River represents the second largest fluvial DOC flux to the ocean at ~ 12.4 Tg C  
202 yr<sup>-1</sup>, or 5% of the global land to ocean flux (Coynel et al., 2005; Spencer et al., 2016). Interestingly,  
203 despite the extensive wetlands in the center of the Congo Basin, the Amazon has a higher DOC

204 yield (4.4 versus 3.4 g C m<sup>-2</sup> yr<sup>-1</sup>), but the organic rich character of both watersheds is apparent  
205 when compared to the global average DOC yield from the world's 30 major rivers (2.3 g C m<sup>-2</sup>  
206 yr<sup>-1</sup>; Raymond and Spencer, 2015). In total, the Amazon River exports ~ 36 Tg C yr<sup>-1</sup> of organic  
207 carbon (OC, both POC and DOC) and the Congo River exports ~14 Tg C yr<sup>-1</sup> to the Atlantic Ocean,  
208 with both rivers exporting OC predominantly as DOC.

209

### 210 **3.4. Floodplain Exchange**

211 The literature on floodplain exchange in the Congo is very sparse, relative to the Amazon. These  
212 floodplains represent regions of significant *in situ* primary production, dominated by  
213 phytoplankton, periphyton, aquatic herbaceous plants, and flooded forests (Sioli 1984; Junk and  
214 Howard-Williamson, 1984; Melack and Forsberg, 2001), and are thought to provide a seasonal  
215 source of organic matter (OM) to the mainstem (Bourgoin et al., 2007; Bonnet et al., 2005). The  
216 contribution of large floating macrophytes, produced primarily in floodplains, may be important  
217 relative to the Basin's overall carbon budget, but the magnitude of their production and export is  
218 highly understudied (Melack and Engle, 2009). During the falling water period, Amazon River  
219 floodplains drain dissolved and particulate material including intact aquatic vegetation (i.e.,  
220 macrophytes) into the mainstem as the floodplains become dry at low water. In addition to  
221 exporting freshly produced OM to the mainstem, productive floodplains can also represent sinks  
222 for sedimentary OM (Moreira-Turcq et al.; 2003). Algal biomass derived from floodplain lakes  
223 and clearwater tributaries has been estimated to represent only 2-8% of Amazon River POC  
224 (Meybeck et al., 1982; Saliot et al., 2001). While they are major bio-reactors in their own right,  
225 the actual magnitude of exchange with the Amazon mainstem remains ambiguous.

226

## 227 **4. Organic Matter Sources and Metabolic Potential**

228 The composition of the OM fractions not only contains signals of not only the origin of the  
229 material, but the potential for degradation by metabolic processes.

230

### 231 **4.1. OM Composition**

232 Discharge is the primary control on POC and DOC export in both the Amazon and Congo  
233 Rivers (Moreira-Turcq et al., 2003; Coynel et al., 2005; Spencer et al., 2016). Concurrent with  
234 elevated concentrations of POC and DOC in the Congo River at high discharge (Figure 2a) a shift  
235 in the source of organic matter is apparent (Spencer et al., 2016). More depleted  $\delta^{13}\text{C}$ -POC and  
236  $\delta^{13}\text{C}$ -DOC values are generally observed with peaks in discharge and along with elevated lignin  
237 carbon-normalized yields ( $\Lambda_8$ ) at these times suggest increasing vascular plant inputs derived from  
238 litters and surface soils. Likewise,  $\Lambda_8$  (total yield of eight lignin-derived phenols indicative of  
239 vascular plant tissues, normalized to weight of bulk sample) for POC is generally highest during  
240 peak discharge both at Óbidos and the river mouth near Macapá, but significant seasonal variability  
241 in the dissolved phase was not observed (Ward et al., 2015).

242 Particulate OM (POM) in the Congo mainstem is comparable to fine particulate OM (FPOM;  
243  $< 63\mu\text{m} > 0.7 \mu\text{m}$ ) in the Amazon at Óbidos with respect to its C:N ratio (9.9-12.4 versus 10.0;  
244 Hedges et al., 1986; 1994) and the Congo River is dominated by FPOM (Spencer et al., 2012;  
245 2016; Figure 2b). Congo River FPOM (C:N 11.4-12.5) is also enriched in nitrogen relative to the  
246 coarse POM (CPOM;  $> 63 \mu\text{m}$ ) fraction (17.2-20.4), as also observed in the Amazon at Óbidos  
247 (20.2) (Hedges et al., 1986; Spencer et al., 2012; Figure 2b). This nitrogen enrichment in the fine  
248 fraction of POM is likely due to nitrogen enriched microbial biomass as well as preferential

249 sorption of nitrogen containing compounds (e.g., amino acids) to the suspended sediments in the  
250 rivers (Aufdenkampe et al., 2001; Marin-Spiotta et al., 2014).

251 Both Congo River  $\delta^{13}\text{C}$ -POC (-26.1 to -28.0 ‰) and  $\delta^{13}\text{C}$ -DOC (-29.0 to -29.8 ‰) reflect the  
252 dominance of terrestrial inputs but with a systematic depletion in  $\delta^{13}\text{C}$ -DOC values due to different  
253 sources between these two components of the OC pool. The enrichment in the  $\delta^{13}\text{C}$ -POC pool may  
254 be due to a variety of factors such as potential phytoplankton inputs or contributions from C4  
255 plants in certain headwaters (Bouillon et al., 2012; Balagizi et al., 2015; Descy et al., 2016). On  
256 the other hand, since POC is typically soil-derived, the relative enrichment of  $\delta^{13}\text{C}$ -POC compared  
257 to  $\delta^{13}\text{C}$ -DOC may be linked to preferential remineralization of  $\delta^{13}\text{C}$  depleted organic carbon in  
258 soils prior to export to the aquatic environment; the older radiocarbon age reported for riverine  
259 POC compared to DOC provides further evidence for this interpretation (Marin-Spiotta et al.,  
260 2014). The depleted signature of  $\delta^{13}\text{C}$ -DOC reflects its source in surface litters and organic-rich  
261 upper soil horizons and also by the predominantly modern radiocarbon age of DOC in major rivers  
262 including the Amazon and Congo Rivers (Mayorga et al., 2005; Spencer et al., 2012; Marwick et  
263 al., 2015). The Congo River  $\delta^{13}\text{C}$ -POC values are comparable to values reported for the Amazon  
264 River at Óbidos (-27.1 to -28.0 ‰; Bouchez et al., 2014), and Congo River  $\delta^{13}\text{C}$ -DOC values are  
265 comparable to those reported for a host of global rivers dominated by terrestrial inputs (Raymond  
266 and Bauer, 2001; Raymond et al., 2007; Mann et al., 2015).

267 A plethora of research in both the Congo and Amazon Rivers has utilized biomarkers to assess  
268 sources of OM (e.g., Hedges et al., 1986; 1994; 2000; Aufdenkampe et al., 2007; Spencer et al.,  
269 2012; 2016). Combining OM C:N and  $\Lambda_8$  has historically been undertaken to examine OM sources  
270 and transformations in both the Congo and Amazon Rivers. Examination of vascular plant  
271 contributions to the OM pool using  $\Lambda_8$  has shown that Congo River POM is high in vascular plant

272 content (2.79 to 3.54 mg 100mg OC<sup>-1</sup>) in comparison to Amazon FPOM at Óbidos (1.68 mg 100mg  
273 OC<sup>-1</sup>) (Hedges et al., 2000; Spencer et al., 2016; Figure 2b). Congo dissolved OM (DOM)  $\Lambda_8$   
274 values (0.50 to 0.76 (mg 100mg OC<sup>-1</sup>) are also high in comparison to major global rivers (Spencer  
275 et al., 2016), highlighting the organic rich nature of the Congo River in both dissolved and  
276 particulate phases.

277

#### 278 **4.2. Degradation Potential of OM**

279  $\Lambda_8$  values from CPOM to FPOM have been attributed to degradative loss of lignin in the source  
280 materials, and dilution with nitrogen enriched microbial and fungal derived OM (Hedges et al.,  
281 1986; Aufdenkampe et al., 2001; Spencer et al., 2016; Figure 2b). When both the Congo and  
282 Amazon River POM C:N and  $\Lambda_8$  data are compared to Mississippi River POM, the organic rich  
283 nature of the tropical systems dominated by terrestrial inputs is apparent. For instance, compared  
284 to the Mississippi River, Amazon River FPOM and Congo River POM  $\Lambda_8$  values are almost double  
285 and roughly three to four times higher, respectively (Figure 2b). This marked terrestrial footprint  
286 has been shown to be an important source of energy fueling the foodweb and critical fisheries in  
287 both the Congo and Amazon Basins (Araujo-Lima et al., 1986; Forsberg et al., 1993; Soto et al.,  
288 2019). Likewise, decomposition of lignin phenols in the Amazon River fuels 30-50% of bulk  
289 microbial respiration in the Amazon River mainstem (Ward et al., 2013). The ratio of lignin acids  
290 to aldehydes (Ad:Al) is an indicator of the decay state of terrestrially-derived OM. The Ad:Al ratio  
291 of POM systematically increases along the lower Amazon River, confirming degradation of POM  
292 in transit (Ward et al., 2015). This downstream shift in degradation state is not as apparent in the  
293 dissolved pool, leading to the hypothesis that DOM is remineralized at similar rates as fresh inputs

294 to the river system from the landscape and floodplains until there is no longer a source, i.e., beyond  
295 the river mouth (see Section 5; Seidel et al., 2015).

296

### 297 **4.3. Deforestation and Agricultural Land-Use Change**

298 Deforestation and forest alteration caused by logging, agricultural expansion, human  
299 settlement, and hunting proceeds at an unrelenting pace throughout the tropics. The epicenter of  
300 tropical deforestation is the Brazilian Amazon Basin, where in recent years an average of ~6,700  
301 km<sup>2</sup> of forest has been lost per year to industrial logging and agricultural land-use change. Recent  
302 rollbacks of environmental protections in Brazil, where more than half of the Amazon's  
303 deforestation occurs, has led to further forest loss by opening new swathes of protected lands to  
304 industrial logging and agriculture. Meanwhile, in the Congo Basin, deforestation continues  
305 similarly unabated, albeit primarily in the form of shifting agriculture (Curtis et al., 2018). Chronic  
306 instability, poor infrastructure, and limited governance in the Congo have so far provided a form  
307 of "passive protection" from the kind of industrial or mechanized deforestation taking place in the  
308 Amazon Basin (De Wasseige et al., 2012). As a result, the rate of forest loss in the Congo Basin  
309 has been relatively lower. However, given the current expansion of mineral extraction, road  
310 development, agribusiness, biofuels, and additional shifting agriculture and charcoal production in  
311 the Congo Basin, its forests may lie at a turning point. Indeed, the population of Democratic  
312 Republic of Congo, the largest country within the Basin, is expected to grow five-fold by 2100  
313 (Gerland et al., 2014). And if recent trends hold, increased mining and infrastructure investments  
314 from China and elsewhere into Central Africa also threaten to accelerate industrial logging. In  
315 short, intensive deforestation promises to be a fixture in both Basins for the foreseeable future.

316 The effect of this rampant tropical deforestation on the local and regional carbon cycle depends  
317 on the original vegetation, soil type, topography, climate, and replacement land-use. Generally,  
318 the net effect of deforestation is to transform ecosystems from a sink into a source of carbon to the  
319 atmosphere through the loss of above-ground biomass, decrease in photosynthetic capacity,  
320 burning of cleared vegetation, and the enhancement of soil carbon respiration.

321 While the loss of carbon as CO<sub>2</sub> released from OC respiration in deforested soils is well  
322 documented, a relatively understudied effect of soil disturbance is the leaching and mobilization  
323 of soil OC (SOC) to rivers and streams. Deforestation has the potential to dramatically augment  
324 this flux in multiple ways. First, the loss of root structure following tree removal destabilizes soils,  
325 leading to erosion and the exposure of deeper, previously stable soil horizons to precipitation.  
326 Second, on the micro to meso-scale (1-100 km<sup>2</sup>), deforestation reduces evapotranspiration and  
327 increases runoff to rivers and streams (Bruijnzeel, 2004; Cavalcante et al., 2019; Costa, 2005).  
328 This post-deforestation increase in the ratio of runoff to precipitation has been observed and  
329 modelled in both the Amazon and Congo Basins (Coe et al., 2009; Drake et al., 2019a; Trancoso,  
330 2006). With more water available to infiltrate into degraded or exposed soil, enhanced leaching of  
331 SOC and rock weathering are likely to increase soil carbon fluxes to streams.

332 In the Amazon, deforestation and agricultural conversion have been shown to impact water,  
333 solute, nutrient, and soil-derived OM export to rivers (Farella et al., 2001; Spencer et al., 2019;  
334 Thomas et al., 2004; Williams and Melack, 1997). Stable carbon isotopic signatures of riverine  
335 DOC and POC in both the Amazon and Congo Rivers exhibit a relative enrichment in deforested  
336 and pasture-influenced catchments, suggesting the export of either soil or C<sub>4</sub>-dominant OC, or  
337 both (Bernardes et al., 2004; Drake et al., 2019a; Richey et al., 1990). Using paired stable and  
338 radiocarbon isotopic measurements can often resolve whether carbon is sourced from modern C<sub>4</sub>

339 plants or aged soil OC (which itself could be originally derived from C4 biomass). In Eastern  
340 Congo, the radiocarbon age of DOC from deforested catchments was found to be ~1,500 years  
341 old, indicating the loss of aged and previously stabilized soil OC from deeper horizons rather than  
342 modern C4-derived vegetation (Drake et al., 2019a).

343 The effect of this mobilization and re-introduction of aged and previously stabilized tropical  
344 SOC into the modern carbon cycle depends, in part, on its composition. Recent studies into the  
345 molecular composition of DOM in both the Amazon and Congo Rivers have uniformly shown that  
346 DOM leached from deforested catchments into rivers is energy-rich (high hydrogen to carbon  
347 ratios) and chemo-diverse (enriched in nitrogen and sulfur compounds) (Drake et al., 2019a; Drake  
348 et al., 2019b; Spencer et al., 2019). The molecular signature of deforestation is readily apparent  
349 when the peak intensities of specific formulae are correlated with the proportion of cropland within  
350 a catchment and plotted in van Krevelen space (Figure 3). Although differences are present, the  
351 overall pattern shows how aliphatic (hydrogen-rich) and reduced (low O/C ratio) DOM (red points,  
352 Figure 3) is strongly correlated with deforestation and consistent across the pan-tropics. Such  
353 compositional signatures are consistent with deeper soil OM, which often contains low-molecular  
354 weight OM sourced from bacteria and stabilized on mineral surfaces (Dungait et al 2012, Lützow  
355 et al. 2006).

356 Together, the carbon isotopic and compositional signatures of deforestation derived DOM in  
357 both the Amazon and Congo Basins indicates microbial bio- or necromass from soils as a source,  
358 given the enriched  $^{13}\text{C}$  and depleted  $^{14}\text{C}$  signatures, high H/C ratios (aliphatic), high N content,  
359 and low aromaticity (Kaiser and Kalbitz, 2012; Kellerman et al., 2018). The ultimate fate of this  
360 mobilized SOC, i.e., whether it is exported downstream to the ocean or mineralized and outgassed  
361 to the atmosphere, depends on its lability and environmental conditions. Bioincubation data from

362 the Eastern Congo show that the aged DOC derived from deforested soils was more biolabile than  
363 younger DOC derived from surface vegetation in the forest and corresponded with higher in-  
364 stream CO<sub>2</sub> concentrations (Figure 4). Assuming that this high biolability is driven primarily by  
365 the highly aliphatic and N-rich chemical composition, as has been observed to be the scenario in  
366 other terrestrial and aquatic systems (Berggren et al., 2010; van Hees et al., 2005; Kalbitz et al.,  
367 2003; Spencer et al., 2015), then we can assume similar patterns of high biolability of OC  
368 mobilized to catchments by deforestation and soil disturbance in both Basins.

369 If tropical deforestation and conversion to agriculture reverses the microbially-mediated  
370 stabilization of OC in soils by venting biolabile and aged OC to the atmosphere via microbial  
371 respiration and outgassing in the aquatic network, then rivers draining impacted landscapes may  
372 represent an important and understudied anthropogenic carbon source. In short, the lateral flux of  
373 disturbed soil carbon to rivers exemplifies an additional mechanism by which deforestation  
374 converts these tropical ecosystems from sinks to sources. For now, this flux appears to be small  
375 relative to the natural fluxes of carbon from tropical rivers, given the modern age of DOC, CO<sub>2</sub>,  
376 and DIC in the mainstem and larger tributaries of the Amazon and Congo Rivers (Hedges et al.,  
377 1986; Marwick et al., 2015; Mayorga et al., 2005; Spencer et al., 2012). Organic matter rich peat  
378 deposits across the majority of Congo wetlands and wetlands in the Peruvian Amazon are another  
379 potential source of aged carbon that is vulnerable to being mobilized into the modern aquatic  
380 carbon cycle due to a variety of disturbances (Dargie et al., 2017; Draper et al., 2014; Moore et al.,  
381 2013). Future work might aim to better quantify the riverine flux of aged OC from deforested  
382 landscapes and to trace its fate downstream before it is masked by mixing with waters draining  
383 pristine or relatively undisturbed areas. In addition to anthropogenic deforestation, the tropical  
384 forest carbon sink in the Amazon is also declining relative to the Congo due to increasing rates of

385 tree mortality linked to hydrologic variability (Hubau et al., 2020). In addition to influencing forest  
386 productivity, hydrologic variability also plays a direct role in the balance between carbon  
387 sequestration in terrestrial environments and mobilization into aquatic ecosystems (Scheffuß, et al.,  
388 2016). For example, model results suggest that while terrestrial net ecosystem productivity and  
389 carbon sequestration is highest during wetter years, the percentage of net primary production lost  
390 to aquatic CO<sub>2</sub> evasion is also highest (Hastie et al., 2019).

391

## 392 **5. Metabolism**

393 The elevated level of pCO<sub>2</sub> even as far as the mouth of such major rivers as the Amazon and  
394 Congo, up to thousands of kilometers from CO<sub>2</sub>-rich small streams, poses a most interesting  
395 question — what set of processes maintains such high levels? The answer is presumably some  
396 combination of instream metabolism of OM of terrestrial and floodplain origin, and/or injection of  
397 high pCO<sub>2</sub> water from local floodplains or tributaries.

398

### 399 **5.1. Metabolic Rates**

400 Metabolic parameters in large rivers are typically measured by dissolved oxygen changes in 60-  
401 ml BOD (Biological Oxygen Demand) bottles over 24 hours, where the bottle is stationary and in  
402 the dark. This technique may inject a critical methodological bias in traditional respiration  
403 experiments—the role of flowing water on biological activity is typically ignored. Ward et al.  
404 (2018a) reported on results from a rotating incubation system that monitors O<sub>2</sub> drawdown in real-  
405 time to evaluate respiration under different flow rates, capable of directly measuring heterotrophic  
406 respiration rates under variable flow velocities. Respiration rates in these rotating chambers were  
407 on the order of 2 to 3 times higher than traditional experiments performed simultaneously, and

408 depth integrated river velocity-normalized respiration rates actually exceeded CO<sub>2</sub> outgassing rates  
409 by ~30%. This excess CO<sub>2</sub> is balanced by new estimates of primary production in the lower  
410 Amazon River based on an O<sub>2</sub> stable isotopic mass balance showing that photosynthesis occurs at  
411 25-50% the rate of respiration (Gagne-Maynard et al., 2017). They conclude that river velocity  
412 and hydrodynamic conditions are key physical factors controlling microbial metabolism of river-  
413 borne OM that has not been appropriately considered either conceptually or quantitatively.  
414 Another important pathway for organic matter remineralization is photo-oxidation and its  
415 interactions with metabolic activity (Cory et al., 2018) are discussed in more detail below.

416 In rivers of the Congo Basin lowlands, Borges et al. (2019) measured primary production (PP)  
417 during 2-hour incubations using <sup>13</sup>C-HCO<sub>3</sub><sup>-</sup> as a tracer and pelagic community respiration (CR)  
418 using the 60 mL BOD bottle technique. On average the PP:CR ratio was 0.28. Volumetric rates of  
419 CR ranged between 0.7 and 46.6 mmol m<sup>-3</sup> d<sup>-1</sup>, while integrated rates of CR ranged between 3  
420 and 790 mmol m<sup>-2</sup> d<sup>-1</sup>. They concluded that CO<sub>2</sub> outgassing was on average about 10 times higher  
421 than the flux of CO<sub>2</sub> produced by aquatic net heterotrophy, indicating that the CO<sub>2</sub> emissions from  
422 the river network were sustained by lateral inputs of CO<sub>2</sub> (either from terra firme or from  
423 wetlands). The authors acknowledge that their CR results might be underestimates based on  
424 finding by Ward et al. (2018a), but consider it unrealistic to assume an underestimation of 10-fold  
425 necessary to bring the balance of CR and PP in balance with outgassing, given that TSS  
426 concentrations are considerably lower in the Congo River than in the Amazon River. However,  
427 Ward et al. (2018a) found the same order of magnitude difference between stationary and rotating  
428 experiments in the clearwater Tapajós River, which has similar TSS levels as the Congo River.

429

## 430 **5.2. Substrates for Metabolism**

431 The previous discussion is underpinned by the concept of rivers no longer being considered  
432 passive pipes (Cole et al., 2007) and opens a new avenue for research: what organic substrates fuel  
433 heterotrophic respiration? Historically, OM in transit in a large river is considered to be stable. But  
434 Ward et al. (2013) showed that the degradation of lignin and associated macromolecules in the  
435 Amazon River corresponds to 30–50% of bulk river respiration. As discussed in the previous  
436 section, these results present strong evidence of the biodegradability of terrestrially derived  
437 macromolecules in the aquatic setting.

438 A process that may be involved is “priming,” whereby the decomposition of less reactive OM  
439 is stimulated by the presence of highly reactive material such as algal exudates. Ward et al. (2016;  
440 2019) showed this potential with the impact of mixing Rios Tapajós and Xingú water in the mixing  
441 zones with the main channel. It is conceivable that this is a pathway by which floodplain waters  
442 could influence respiration in the main channel. Another potential fuel for river respiration and  
443 direct source of CO<sub>2</sub> to tropical waters are the by-products of photo-oxidized OM.

444 Terrestrially derived OM in tropical rivers can be subject to intense solar radiation, which can  
445 directly oxidize organic compounds to CO<sub>2</sub> and photodegrade other aromatic compounds into  
446 potentially more biolabile forms. Indeed, irradiation experiments conducted on Congo River water  
447 produced new compounds that were highly aliphatic (hydrogen-rich), a characteristic common to  
448 highly biodegradable OM (Stubbins et al. 2010). Initial conservative estimates suggest that photo-  
449 oxidation only contributes to ~0.5% of CO<sub>2</sub> emission rates in the Amazonian Negro River  
450 (Remington et al., 2011). Other experiments in the Negro River have shown that solar irradiation  
451 contributes to ~7% of DOC mineralization in tropical blackwater systems and that exposure to  
452 sunlight produces bio-labile DOC, stimulating microbial respiration (Amaral et al. 2013). Along  
453 the lower reaches of the Amazon River mainstem, rates of dissolved lignin decay via photo-

454 oxidation are on the same order of magnitude as microbial degradation (Ward et al., 2013; Seidel  
455 et al. 2016). However, a remaining challenge is quantifying the importance of depth-integrated  
456 photo-oxidation across the diversity of river types. For example, the abundance of suspended  
457 sediments in the deep channels of the Amazon River mainstem likely limit the importance of  
458 photo-oxidation, while photo-oxidation may play a significant role in transforming OM in less  
459 turbid systems such as Amazonian clearwater tributaries.

460 Other potential sources of  $p\text{CO}_2$  in the mainstem rivers could be direct inputs from soils or the  
461 injection from floodplains of high  $p\text{CO}_2$  directly, or DOC and POC as substrates for riverine  
462 respiration. While the majority of  $\text{CO}_2$  emissions from headwater streams is derived from soil  
463 respiration (Johnson et al., 2008), contributions from this pathway diminish at increasing stream  
464 orders (Raymond et al., 2016). With respect to floodplain  $\text{CO}_2$  contributions to the main river  
465 channel, Abril et al. (2014) developed a simple one-dimensional model that simultaneously  
466 calculates the floodplain-derived  $\text{CO}_2$  lost by outgassing and the  $\text{CO}_2$  that remains dissolved in  
467 water and is transported downstream based on extensive measurements across the floodplain and  
468 mainstem in different locations. Their model computed that water movement is fast enough  
469 relative to gas exchange to maintain high supersaturation of the floodplain  $p\text{CO}_2$  over dozens to  
470 hundreds of kilometers without requiring heterotrophic metabolism. They estimated that  
471 Amazonian wetlands export half of their GPP to river waters as dissolved  $\text{CO}_2$  and OC, compared  
472 with only a few percent of GPP exported in upland (non-flooded) ecosystems, concluding that the  
473 input of strictly upland terrestrial carbon to river  $\text{CO}_2$  outgassing is potentially minor compared to  
474 the wetland carbon contribution. A similar argument is made for the Congo (Borges et al. 2019).

475 That said, it is not clear what the impacts of the floodplain export to the main channel actually  
476 are. To be significant, a mass balance (e.g., NEE) has to be demonstrated, on the flux to, by season,

477 relative to the mass being transported in the river; i.e., how many  $\text{m}^3 \text{s}^{-1}$  of water with what  
478 chemical load is being exported to the mass of the main river? Alsdorf et al (2010) computed that  
479 water stored on and subsequently drained from the mainstem Amazon floodplain each year  
480 represents only about 5% of the total volume of water discharged from the Amazon River, and  
481 that the contribution to the floodplain from local upland runoff represents less than 20% of the  
482 floodplain water volume for any given time. The Abril et al. (2014) model tracks only a parcel of  
483 water from the floodplain, not accounting for the mass of water and the  $\text{pCO}_2$  of the main channel.  
484 Further, the assumption that heterotrophic respiration in the main channel is much less than  
485 outgassing, hence requiring lateral inputs, is based in large part on the classic BOD bottle  
486 techniques. Most all previous balances using respiration measured with the classic small bottle  
487 need re-evaluation, in light of the Ward et al. (2018a) results.

488

## 489 6. Gas Exchange

490 As summarized by Melack (2016), gas exchange between surficial water and overlying  
491 atmosphere depends on the concentration gradient between air and water and on physical processes  
492 at the interface, usually parameterized as a gas transfer velocity ( $k_{600}$ ), also called a piston velocity  
493 or gas exchange coefficient:  $F_{\text{CO}_2} = k_{600} (C_s - C_o)$ , where  $F$  is the evasive flux,  $C_s$  is the surface  
494 water concentration, and  $C_o$  is the atmospheric equilibrium. The challenge is that  $k_{600}$  varies widely  
495 and is difficult to measure directly. Melack (2016) and MacIntyre et al. (2019) summarized direct  
496 techniques involving floating chambers, surface renewal models, eddy covariance, and tracers  
497 such as  $^{222}\text{Rn}$ . The measurement is especially problematic on large rivers. Studies frequently  
498 default to literature or modelled values for  $k_{600}$ . It should also be noted that  $k_{600}$  and  $\text{pCO}_2$  may not  
499 be entirely independent. For example, highly elevated  $\text{pCO}_2$  levels (e.g.,  $> 20,000 \mu\text{atm}$ ) are

500 generally only observed in settings with low  $k_{600}$  values (e.g., floodplains) due to gas exchange  
501 limitations. On the other hand, turbulent settings with high  $k_{600}$  values typically do not become  
502 highly saturated in  $p\text{CO}_2$  as exchange occurs more rapidly than production (Rocher-Ros et al.,  
503 2019).

504 For the Congo River, Borges et al. (2019) used a parameterization for  $k_{600}$  of stream slope and  
505 stream water velocity, as a function of Strahler stream order, where  $k_{600}$  becomes smaller as stream  
506 order gets larger. Computed values were in the range of 12-30  $\text{cm hr}^{-1}$  for streams greater than  
507 stream order 3, generally in the range reported by Alin et al. (2011), for the Amazon and Mekong  
508 rivers. The calculated  $F_{\text{CO}_2}$  ranged between 86 and 7,110  $\text{mmol m}^{-2} \text{d}^{-1}$ , averaging 2,500  $\text{mmol}$   
509  $\text{m}^{-2} \text{d}^{-1}$  (weighted by surface area of Strahler stream order). The  $F_{\text{CO}_2}$  decreased with increasing  
510 Strahler order. Strahler orders 1–4 accounted for > 90 % of the integrated  $F_{\text{CO}_2}$ , while Strahler  
511 orders 5–10 only accounted for 9.3% of integrated  $F_{\text{CO}_2}$ . The rivers draining the Cuvette Central  
512 contributed to 6 % of the basin-wide emissions for  $\text{CO}_2$ .

513 For the Amazon, Melack (2016) summarizes a wide range of  $k_{600}$  and outgassing fluxes across  
514 different Amazonian environments, from small streams to flooded lakes to large rivers. Values  
515 ranged from 40  $\text{mmol m}^{-2} \text{d}^{-1}$  to 6,700  $\text{mmol m}^{-2} \text{d}^{-1}$ . For the lower Amazon, i.e., Óbidos to  
516 Macapá, Sawakuchi et al. (2017) estimated an average  $k_{600}$  (based on direct measurements of fluxes  
517 and concentrations) for all stations of  $34 \pm 16 \text{ cm hr}^{-1}$ , slightly higher than the maximum Congo  
518 River  $k_{600}$  values computed by Borges et al. (2019). Sawakuchi et al. (2017, corrigendum)  
519 calculated the total flux of  $\text{CO}_2$  from the main channel of the lower Amazon River from Óbidos to  
520 Macapá, which had an average wetted surface area of 7,118  $\text{km}^2$ , as 0.02  $\text{Pg C yr}^{-1}$ . They then  
521 extrapolated from Macapá to the actual river mouth, which has an additional surface area of 11,261  
522  $\text{km}^2$ , producing a  $\text{CO}_2$  flux of 0.03  $\text{Pg C yr}^{-1}$ . The sum of fluxes for these two zones, or the total

523 emissions from Óbidos to the actual river mouth was  $0.05 \text{ Pg C yr}^{-1}$ . This flux is roughly 10% of  
524 the first estimations of  $\text{CO}_2$  outgassing from the entire Amazon River Basin that conservatively  
525 extrapolated measurements from the central Amazon River (Richey et al., 2002).

526 Overall, it is clear that the original Richey et al. (2002) estimate of  $0.5 \text{ Pg C yr}^{-1}$  is a considerable  
527 underestimate of total outgassing from the aquatic habitats of the Amazon Basin. Re-evaluating  
528 new data and understanding, Melack (2016) estimated an updated value for annual  $\text{CO}_2$  emission  
529 from aquatic habitats in the lowland Amazon Basin of  $1.8 \text{ Pg C yr}^{-1}$ , with 90% of this flux likely  
530 being associated with lakes, floodplains, and other wetlands. It does not include Sawakuchi et al.  
531 (2017) calculations for the lower river to the mouth, nor does it include likely outgassing from the  
532 Amazon plume, as the  $\text{CO}_2$ -rich water enters the ocean. Borges et al. (2019) gives an updated  
533 integrated  $\text{CO}_2$  outgassing flux for the Congo River network of  $0.25 \pm 0.05 \text{ Pg C yr}^{-1}$ . They  
534 conclude that the primary sources are almost certainly not terrestrial carbon being decomposed in  
535 the river, with the most likely alternative source being wetlands (flooded forest and aquatic  
536 macrophytes).

537

## 538 **7. The River-to-Ocean Continuum**

539 Unsurprisingly, both plumes of the Amazon and Congo Rivers exert a strong influence onto the  
540 Atlantic Ocean and, as highlighted earlier, export substantial amounts of terrestrially derived  $\text{pCO}_2$   
541 and OM. Here we consider their respective marine fates.

542

### 543 **7.1. Marine Fate of Riverine $\text{CO}_2$**

544 Do signals of elevated river  $\text{pCO}_2$  then propagate beyond the mouth of large rivers? Integrated  
545 *in situ* measurements at the mouth of the Amazon River and out into the plume with satellite

546 observations from the Soil Moisture and Ocean Salinity (SMOS) satellite suggest that, including  
547 the plume area near the mouth, the plume is a net source of CO<sub>2</sub>, with an average annual flux of  
548  $5.6 \pm 7.2 \text{ Tg C y}^{-1}$  (Valerio et al., in press; Ward et al., 2018b). This is contrary to past studies (e.g.,  
549 Cooley et al., 2007; Ibánhez et al., 2015) that estimated the region to be a net sink of atmospheric  
550 CO<sub>2</sub>. The inclusion of lower salinity waters has shifted these estimates to near net neutral (Valerio  
551 et al., in press). This calculation is likely an underestimate, as SMOS coverage is not valid within  
552 100 km offshore. Intra-annual variability was related to discharge patterns at the river mouth and  
553 ocean currents plus trade winds in the plume, as a consequence of climatic events such as the  
554 severe drought throughout the Amazon Basin in 2010, and record flood in 2012-2014. The  
555 immediate question is, how far does the extension of the Congo plume result in CO<sub>2</sub> outgassing  
556 and at what magnitude? In the case of the Amazon, freshwaters extend up to 100 km beyond the  
557 actual river mouth, covering a significant amount of surface area relative to the river channel  
558 (Sawakuchi et al., 2017).

559 The previous discussion highlights a critical gap in observational data—the nearshore plume  
560 environments of large rivers, which are logistically difficult to measure. While oceanographic  
561 cruises typically do not make measurements directly adjacent to river mouths, river studies  
562 typically do not extend beyond the river mouth. These observational gaps are a byproduct of both  
563 logistical constraints and traditional disciplinary boundaries not crossed by limnologists and  
564 oceanographers until relatively recently. Addressing this gap requires careful collaboration  
565 between riverine and marine scientists, and nimble research vessels capable of sampling in these  
566 difficult nearshore regions. Great progress has been made in this regard over the last several  
567 decades and we advocate for increased efforts to sample across the river-ocean continuum.

568

## 569 7.2. Marine Fate of Organic Matter

570 Historic estimates of the residence time of terrestrial DOM in the Atlantic Ocean were derived  
571 from lignin concentrations measured in the open ocean and scaling average lignin fluxes from the  
572 Amazon and Mississippi Rivers to all other rivers draining into the Atlantic Ocean (Opsahl and  
573 Benner, 1997; Hernes and Benner, 2006). However, both the Amazon and Mississippi exhibit  
574 lower  $\Lambda_8$  values than the Congo River (i.e., they are not as efficient at exporting lignin per mg of  
575 DOC as the Congo). Additionally, the Congo River is more efficient than the Amazon River at  
576 exporting lignin per unit volume as the Congo exports ~ 50% of the lignin load in ~ 20% of the  
577 volume of the Amazon River at Óbidos (i.e., 2.5 times more efficient) (Spencer et al., 2016). If the  
578 Congo River flux of dissolved lignin is extrapolated to the freshwater input of the Atlantic Ocean,  
579 the result is a much-reduced residence time for terrestrial DOM (~ 13 years versus ~ 35 years).  
580 Although it is unrealistic to extrapolate the Congo River lignin flux data to all other Atlantic Ocean  
581 draining rivers, this clearly highlights the sensitivity to the original calculations derived solely  
582 from the Amazon and Mississippi rivers, and emphasizes the disproportionate role organic rich  
583 systems like the Congo can play on overall ocean residence time estimates (Spencer et al., 2016).  
584 Regardless of how these lignin fluxes are represented, the residence time of terrestrial DOM is  
585 substantially lower than the mixing time of the world's oceans (500-1000 years) and apparent age  
586 of bulk DOC in the ocean (4,000 to 6,000 years; Williams and Druffel, 1987).

587 With respect to the fate of Amazon River DOM in the Atlantic Ocean, recent research suggests  
588 that a large fraction is stable over the continental margin, potentially due to extensive prior  
589 biodegradation in soils and the Amazon fluvial network (Ward et al., 2013; Medeiros et al., 2015;  
590 Seidel et al., 2015). Also, Amazon River plume waters are exported from the continental margin  
591 quickly ( $\leq 2$  months) and thus a major fraction may survive export across the margin due to the

592 short residence time, particularly as this is coupled with high TSS concentrations that decreases  
593 photo-oxidation (Medeiros et al., 2015). Conversely with respect to the Congo River, the low TSS  
594 concentrations, its outflow position near the Equator, and its extensive surface plume in which  
595 Congo freshwater has been shown to be confined to the surface 15 m for the initial 200 km of the  
596 plume, and low salinity waters extend for 700 to 800 km from the mouth provide an ideal location  
597 for photo-oxidation (Eisma and Van Bennekom, 1978; Pak et al., 1984; Spencer et al., 2009). To  
598 date the proportion of DOC exported from the Congo River that is photo-mineralized remains  
599 unknown, but laboratory based photo-oxidation experiments have shown loss of ~ 45 % of Congo  
600 River DOC with simulated sunlight (Spencer et al., 2009). As discussed previously, these  
601 experiments also changed the composition of Congo River DOM, preferentially degrading the  
602 chromophoric fraction (CDOM) and lignin, enriching the  $\delta^{13}\text{C}$ -DOC toward marine endmember  
603 values and shifting the molecular composition of DOM toward a less condensed, less aromatic  
604 composition (Spencer et al., 2009; Stubbins et al., 2010). This selective removal of the  
605 characteristics of terrestrial DOM resulted in a photo-resistant and altered pool that although  
606 sourced from the Congo would be difficult to trace back to its origins.

607 The fate of POM exported by the Amazon River has been well-studied and highlights low  
608 preservation of OM in high energy, mobile muds that receive extensive oxygen exposure and are  
609 home to diverse microbial communities (Hedges et al., 1997; Blair and Aller, 2012). At the mouth  
610 of the Congo River, the Congo Canyon facilitates burial of POC to the abyssal plain. Recent studies  
611 underscore efficient transport from the Canyon to the Congo Fan and across the depocenter a fan-  
612 wide deposition rate of  $\sim 0.7 \text{ Tg C yr}^{-1}$ , and a burial rate of  $\sim 0.4 \text{ Tg C yr}^{-1}$  (Rabouille et al., 2009;  
613 Savoye et al., 2009). Comparing this to the Congo River POC flux of  $2 \text{ Tg C yr}^{-1}$  suggests that ~  
614 36 % of exported POC reaches the depocenter and approximately one-fifth is ultimately buried

615 (Spencer et al., 2016). When compared to depocenters with extensive particle residence time in  
616 oxygenated waters like the Amazon and Mississippi which exhibit greater remineralization of POC  
617 (Aller et al., 1996; Allison et al., 2007) it is apparent the Congo River is a highly efficient site of  
618 POC preservation. Thus despite its comparably low POC flux, ultimately the Congo represents a  
619 sizeable fraction of the estimated POC burial term for the South Atlantic ( $\sim 1.8 \text{ Tg C yr}^{-1}$ ;  
620 Mollenhauer et al., 2004) and even of global deep-sea POC burial (10-20  $\text{Tg C yr}^{-1}$ ; Berner, 1989;  
621 Hedges and Keil, 1995) due to the efficient injection of POC via the Congo Canyon to the Congo  
622 Fan.

623

## 624 **8. Conclusion**

625 Together the Amazon and Congo represent the end-member of the River Continuum (*sensu*  
626 Vannote et al., 1980), and illustrate the important role of fluvial systems in the global carbon cycle.  
627 Examining the interdependence of  $\text{pCO}_2$ , DOM, and POM within the construct of NEE in these  
628 large aquatic systems, while incomplete, provides a quantitative perspective on the dynamics of  
629 the respective C fractions.

630 A major difference between the basins, other than size and rainfall regime, is that the Amazon  
631 has origins in the high Andes, producing a much higher sediment load than the Congo. But organic  
632 loading on the sediments is  $\sim 5\text{x}$  greater in the Congo than the Amazon, so the total flux of OM in  
633 the Amazon is only  $\sim 3\text{x}$  greater than the Congo despite the fact that the Amazon discharges  $\sim 5\text{x}$   
634 as much water. Hydrology governs carbon in both rivers, with both the greatest concentration of  
635 dissolved and particulate carbon at high water, and with biomarkers indicating increasing vascular  
636 plant inputs derived from litters and surface soils relative to low water. While the  $\delta^{13}\text{C}$  and C:N  
637 signatures of OM between the two rivers are comparable,  $\Lambda_8$  values indicate that the vascular plant

638 contribution to POM in the Congo is  $\sim 2x$  greater than in the Amazon. Overall, the organic rich  
639 nature of the tropical systems dominated by terrestrial inputs is readily apparent, especially  
640 compared to the Mississippi River and other global rivers. Landuse change in both basins leads to  
641 changes in the molecular composition of POM from deeper soil horizons and DOM leached from  
642 deforested catchments in both the Amazon and Congo Rivers. These energy-rich OM sources  
643 would presumably be more reactive in oxygenated river settings compared to deep soil  
644 environments, leading to enhanced metabolism and reintroduction of pre-aged carbon into the  
645 modern carbon cycle.

646 Terrestrially-derived OM feeds foodwebs in both the Congo and the Amazon, from fisheries to  
647 microbes. Decomposition of lignin phenols during transit appears to support a significant  
648 percentage of in situ respiration in the Amazon. While data are lacking, it would be reasonable to  
649 assume the same for the organic-rich Congo River. The process of priming may also expedite this  
650 OM remineralization. Combined with recent measurements indicating that traditional static BOD  
651 bottle measured respiration produces results 2-3x lower than more realistic rotating chambers  
652 suggests that in situ respiration may play a major role in sustaining the high levels of  
653 supersaturation of  $pCO_2$  far downriver. In the lowermost Amazon,  $pCO_2$  begins to decrease, with  
654 turbulence from winds and tides.

655 The marine fate of the river-borne materials is quite different. The Congo Canyon facilitates  
656 burial of POM to the abyssal plain. In contrast, POM exported by the Amazon River is minimally  
657 preserved in the high energy, mobile muds of the plume that receive extensive oxygen exposure.  
658 A large fraction of DOM is stable over the continental margin, potentially due to extensive prior  
659 biodegradation in soils and the Amazon fluvial network, and short residence time across the shelf.  
660 DOM exported by the low-sediment Congo River is subject to considerably more photooxidation

661 and selective removal of terrestrial signals. The greater fraction of lignin in the Congo relative to  
662 the Amazon and Mississippi leads to estimates of reduced residence time for terrestrial DOM.  
663 Depending on the season, the CO<sub>2</sub> discharged by the Amazon River into the plume persists to the  
664 extent that the plume can be considered a net source, rather than sink, of pCO<sub>2</sub>. Comparable data  
665 are not available for the Congo.

666 Based on the data summarized here, it would appear that the Alsdorf et al. (2016) hypothesis  
667 that the annual-average amount of CO<sub>2</sub> evasion from the Congo Basin is greater than the Amazon  
668 per unit area is not supported. As was the case with the Amazon, further information in this data-  
669 sparse region would certainly modify these results, both for magnitude and possibly for dynamics.  
670 Regardless of absolute magnitude the key finding with the Congo is that it too is a highly dynamic  
671 region of aquatic carbon cycling. It is too early to conclude how these outgassing results relate to  
672 the overall carbon balance of these largest river basins, and how this carbon balance will shift  
673 under future scenarios. Model results suggest that the export of carbon and emission of CO<sub>2</sub> from  
674 the Amazon River vary systematically with climate (e.g., more CO<sub>2</sub> evasion during wet years;  
675 Hastie et al., 2019) and that these fluxes have steadily increased by ~25 % since 1861 in the Congo  
676 River (Hastie et al., 2020). However, such representation of river and coastal carbon fluxes are not  
677 currently deployed in global scale models, limiting our ability to interpret potential feedbacks  
678 among these interconnected components of the Earth system (Ward et al., 2020). Thus,  
679 disentangling the natural drivers of large riverine carbon cycling remains a challenge, and the  
680 complexity and importance of this effort is becoming increasingly compounded by human  
681 disturbances discussed. One interpretation is that there is an aquatic-based carbon cycle that is not  
682 accounted for in terrestrially focused carbon budgets.

683

684 **References**

- 685 Abril, G., Martinez, J.-M., Artigas, L.F., Moreira-Turcq, P., Benedetti, M.F., Vidal, et al. (2014).  
686 Amazon River carbon dioxide outgassing fuelled by wetlands. *Nature* 505: 395–398.  
687 doi:10.1038/nature12797
- 688 Alin, S. R., M.D.F.L. Rasera, C. I. Salimon, J. E. Richey, G. W. Holtgrieve, A. V. Krusche, and  
689 A. Snidvongs. (2011). Physical controls on carbon dioxide transfer velocity and flux in low-  
690 gradient river systems and implications for regional carbon budgets. *Journal of*  
691 *Geophysical Research. Biogeosciences*. 116:G01009. doi:10.1029/2010JG001398
- 692 Allen, G. H., and Pavelsky, T. M. (2018). Global extent of rivers and streams. *Science*, 361(6402),  
693 585-588.
- 694 Aller, R.C., Blair, N.E., Xia, Q. and Rude, P.D. (1996). Remineralization rates, recycling, and  
695 storage of carbon in Amazon shelf sediments. *Continental Shelf Research*, 16(5-6), pp.753-786.
- 696 Allison, M.A., Bianchi, T.S., McKee, B.A. and Sampere, T.P. (2007). Carbon burial on river-  
697 dominated continental shelves: Impact of historical changes in sediment loading adjacent to the  
698 Mississippi River. *Geophysical Research Letters*, 34(1).
- 699 Alsdorf, D., Han, S-C., Bates, P., and Melack, J. (2010). Seasonal water storage on the Amazon  
700 floodplain measured from satellites. *Remote Sensing of Environment* 114: 2448-2456.
- 701 Alsdorf, D., Beighley, E., Laraque, A., Lee, H., Tshimanga, R., O’Loughlin, F., Mahé, G., Dinga,  
702 B., Moukandi, G., and Spencer, R. (2016), Opportunities for hydrologic research in the Congo  
703 Basin, *Rev. Geophys.*, 54, doi:10.1002/2016RG000517.
- 704 Amaral, J. H. F., Suhett, A. L., Melo, S., and Farjalla, V. F. (2013). Seasonal variation and  
705 interaction of photodegradation and microbial metabolism of DOC in black water Amazonian  
706 ecosystems. *Aquatic Microbial Ecology*, 70(2), 157-168.

- 707 Amaral, J.H.F., Farjalla, V.F., Melack, J.M., Kasper, D., Scofield, V., Barbosa, P.M., and  
708 Forsberg, B.R. (2019). Seasonal and spatial variability of CO<sub>2</sub> in aquatic environments of the  
709 central lowland Amazon basin. *Biogeochemistry* 143:133–149.
- 710 Araújo, K.R., Sawakuchi, H., Bertassoli Jr, D.J., Sawakuchi, A.O., da Silva, K.D., Vieira, T.B.,  
711 Ward, N.D. and Pereira, T.S. (2019). Carbon dioxide (CO<sub>2</sub>) concentrations and emission in the  
712 newly constructed Belo Monte hydropower complex in the Xingu River, Amazonia.  
713 *Biogeosciences*, 16(18), pp.3527-3542.
- 714 Araujo-Lima, C.A.R.M., Forsberg, B.R., Victoria, R., Martinelli, L. (1986) Energy sources for  
715 detritivorous fishes in the Amazon. *Science*, 234, 1256-1258.
- 716 Aufdenkampe, A.K., Hedges, J.I., Richey, J.E., Krusche, A.V., and Llerena, C.A. (2001) Sorptive  
717 fractionation of dissolved organic nitrogen and amino acids onto fine sediments within the  
718 Amazon Basin. *Limnology and Oceanography*, 46, 1921-1935.
- 719 Aufdenkampe, A.K., Mayorga, E., Hedges, J.I., Llerena, C.A., Quay, P.D., Gudeman, J., Krusche,  
720 A.V., and Richey, J.E. (2007) Organic matter in the Peruvian headwaters of the Amazon:  
721 Compositional evolution from the Andes to the lowland Amazon mainstem. *Organic*  
722 *Geochemistry*, 38, 337-364.
- 723 Balagizi, C.M., Darchambeau, F., Bouillon, S., Yalire, M.M., Lambert, T., Borges, A.V. (2015)  
724 River geochemistry, chemical weathering, and atmospheric CO<sub>2</sub> consumption rates in the  
725 Virunga Volcanic Province (East Africa). *Geochemistry, Geophysics, Geosystems*, 16, 2637-  
726 2660.
- 727 Barbosa, P.M., Melack, J.M., Amaral, J.H.F., Scofield, V., Farjalla, V., and Forsberg, B.R.  
728 (2016). Methane concentrations and fluxes from rivers and lakes in the Amazon basin.  
729 *Limnology and Oceanography* 61, S221-237.

- 730 Barbosa, P.M., Melack, J.M., Amaral, J.H.F., MacIntyre, S., Kasper, D., Cortes, A.C., Farjalla  
731 V.F., and Forsberg, B.R. (2020). Dissolved CH<sub>4</sub> concentrations and fluxes to the atmosphere  
732 from a tropical floodplain lake. *Biogeochemistry*, [doi.org/10.1007/s10533-020-00650-1](https://doi.org/10.1007/s10533-020-00650-1).
- 733 Berggren, M., Laudon, H., Haei, M., Ström, L., and Jansson, M. (2010). Efficient aquatic bacterial  
734 metabolism of dissolved low-molecular-weight compounds from terrestrial sources. *The ISME*  
735 *Journal*, 4(3), 408–416.
- 736 Bernardes, M. C., Martinelli, L. A., Krusche, A. V., Gudeman, J., Moreira, M., Victoria, R. L., et  
737 al. (2004). Riverine organic matter composition as a function of land use changes southwest  
738 Amazon. *Ecological Applications* 14(sp4), 263–279.
- 739 Berner, R.A. (1989), Biogeochemical cycles of carbon and sulfur and their effect on atmospheric  
740 oxygen over phanerozoic time. *Global and Planetary Change* (1): 97-122.  
741 [doi.org/10.1016/0921-8181\(89\)90018-0](https://doi.org/10.1016/0921-8181(89)90018-0)
- 742 Blair, N.E., and Aller (2012), The fate of terrestrial organic carbon in the marine environment.  
743 *Annual Review of Marine Science*, 4, 401-423.
- 744 Bonnet, M.-P., G. Barroux, P. Seyler, G. Peclý, P. Moreira-Turcq, C. Lagane, G. Cochoneau, J.  
745 Viers, F. Seyler, and J.-L. Guyot (2005), Seasonal links between the Amazon corridor and its  
746 flood plain: The case of the varzea of Curuai, in Dynamics and Biogeochemistry of River  
747 Corridors and Wetlands, *Proceedings of symposium S4 held during the Seventh IAHS Scientific*  
748 *Assembly* at Foz do Iguaçu, Brazil, April 2005), IAHS Publ., 294.
- 749 Borges, A., G. Abril, F. Darchambeau, C.R. Teodoru, J., Deborde, L.O. Vidal, T. Lambert, and S.  
750 Bouillon (2015), Divergent biophysical controls of aquatic CO<sub>2</sub> and CH<sub>4</sub> in the world's two  
751 largest rivers. *Scientific Reports*, 5, 15614.
- 752 Borges, A.V., Darchambeau, F., Lambert, T., Morana, C., Allen, G.H., Tambwe, E., Sembaito,

- 753 A.T., Mambo, T., Wabakhangazi, J.N., Descy, J-P, Teodoru, C.R. and Bouillon, S. (2019).  
754 Variations in dissolved greenhouse gases (CO<sub>2</sub>, CH<sub>4</sub>, N<sub>2</sub>O) in the Congo River network  
755 overwhelmingly driven by fluvial-wetland connectivity. *Biogeosciences*, 16, 3801–3834,  
756 <https://doi.org/10.5194/bg-16-3801-2019>
- 757 Bouchez, J., Galy, V., Hilton, Gaillardet, J., Moreira-Turcq, P., Perez, M.A., France-Lanord, C.,  
758 and Maurice (2014), Source, transport and fluxes of Amazon River particulate organic carbon:  
759 Insights from river sediment depth-profiles. *Geochimica et Cosmochimica. Acta*, 133, 280-298.
- 760 Bouillon, S., Yambélé, A., Spencer, R.G.M., Gillikin, D.P., Hernes, P.J., Six, J., et al. (2012).  
761 Organic matter sources, fluxes and greenhouse gas exchange in the Oubangui River (Congo  
762 River Basin). *Biogeosciences* 9, 2045–2062.
- 763 Bourgoïn, L.M., Bonnet, M.P., Martinez, J-M, Kosuth, B., Cochonnea, G., Moreira-Turcq, B.,  
764 Guyot, J-L., Vauchele, P., Filizola, N., and Seyler, P. (2007). Temporal dynamics of water and  
765 sediment exchanges between the Curuai floodplain and the Amazon River, Brazil. *Journal of*  
766 *Hydrology* 335, 140–156.
- 767 Bruijnzeel, L. A. (2004). Hydrological functions of tropical forests: not seeing the soil for the  
768 trees? *Agriculture, Ecosystems and Environment*, 104(1), 185–228.
- 769 Butman, D., and Raymond, P. (2011). Significant efflux of carbon dioxide from streams and rivers  
770 in the United States. *Nature Geoscience*. DOI: 10.1038/NGEO1294
- 771 Cavalcante, R. B. L., Pontes, P. R. M., Souza-Filho, P. W. M., and Souza, E. B. (2019). Opposite  
772 Effects of Climate and Land Use Changes on the Annual Water Balance in the Amazon Arc of  
773 Deforestation. *Water Resources Research*, 55(4), 3092–3106.
- 774 Coe, M. T., Costa, M. H., and Soares-Filho, B. S. (2009). The influence of historical and potential  
775 future deforestation on the stream flow of the Amazon River--Land surface processes and

- 776 atmospheric feedbacks. *Journal of Hydrology*, 369(1-2), 165–174.
- 777 Cole, J. J., Pace, M.L., Carpenter, S.R., Kitchell, J.F. (2000). Persistence of Net Heterotrophy in  
778 Lakes during Nutrient Addition and Food Web Manipulations. *Limnology and Oceanography*.  
779 45 (8), 1718-1730
- 780 Cole, J. J., Prairie, Y. T., Caraco, N. F., McDowell, W. H., Tranvik, L. J., Striegl, R. G., et al.  
781 (2007). Plumbing the global carbon cycle: integrating inland waters into the terrestrial carbon  
782 budget. *Ecosystems*, 10(1), 172-185.
- 783 Cooley, S.R., Coles, V.J., Subramaniam, A. and Yager, P.L. (2007). Seasonal variations in the  
784 Amazon plume-related atmospheric carbon sink. *Global Biogeochemical Cycles*, 21(3).
- 785 Cory, R. M., Ward, C. P., Crump, B. C., and Kling, G. W. (2014). Sunlight controls water column  
786 processing of carbon in arctic fresh waters. *Science*, 345(6199), 925-928.
- 787 Costa, M. H. (2005). Large-scale hydrological impacts of tropical forest conversion. Pp. 590-597.  
788 In M. Bonell and L. A. Bruijnzeel (eds), *Forests, Water and People in the Humid Tropics*,  
789 Cambridge University Press.
- 790 Coynel, A., Seyler, P., Etcheber, H., Meybeck, M., and Orange, D. (2005), Spatial and seasonal  
791 dynamics of total suspended sediment and organic carbon species in the Congo River. *Global*  
792 *Biogeochemical Cycles* 19, GB4019, doi:10.1029/2004GB002335.
- 793 Curtis, P. G., Slay, C. M., Harris, N. L., Tyukavina, A., and Hansen, M. C. (2018). Classifying  
794 drivers of global forest loss. *Science*, 361(6407), 1108–1111.
- 795 Dargie, G. C., Lewis, S. L., Lawson, I. T., Mitchard, E. T., Page, S. E., Bocko, Y. E., and Ifo, S.  
796 A. (2017). Age, extent and carbon storage of the central Congo Basin peatland complex. *Nature*,  
797 542(7639), 86-90.
- 798 De Wasseige, C., De Marcken, P., Bayol, N., Hiol, F., Mayaux, P., Desclée, B., et al. (eds) (2012).

- 799 The forests of the Congo basin: state of the forest 2010. Publications Office of the European  
800 Union. Luxembourg. 276 p. ISBN: 978-92-79-22716-5, doi:10.2788/47210
- 801 Descy, J.P., Darchambeau, F., Lambert, T., Stoyneva-Gaetner, M.P., Bouillon, S., Borges, A.V.  
802 (2016). Phytoplankton dynamics in the Congo River. *Freshwater Biology*, 62, 87-101.
- 803 Drake, T.W., Raymond, P.A. and Spencer, R.G.M. (2017). Terrestrial carbon inputs to inland  
804 waters: A current synthesis of estimates and uncertainty. *Limnology and Oceanography Letters*  
805 <https://doi.org/10.1002/lol2.10055>
- 806 Drake, T. W., Podgorski, D. C., Dinga, B., Chanton, J., Six, J., and Spencer, R. G. M. (2019a).  
807 Land-use controls on carbon biogeochemistry in lowland streams of the Congo Basin. *Global*  
808 *Change Biology*. <https://doi.org/10.1111/gcb.14889>
- 809 Drake, T. W., Van Oost, K., Barthel, M., Bauters, M., Hoyt, A. M., Podgorski, D. C., et al. (2019b).  
810 Mobilization of aged and biolabile soil carbon by tropical deforestation. *Nature Geoscience*,  
811 12(7), 541–546.
- 812 Draper, F. C., Roucoux, K. H., Lawson, I. T., Mitchard, E. T., Coronado, E. N. H., Lähteenoja, O.,  
813 et al. (2014). The distribution and amount of carbon in the largest peatland complex in  
814 Amazonia. *Environmental Research Letters*, 9(12), 124017.
- 815 Dungait, J. A., Hopkins, D. W., Gregory, A. S., and Whitmore, A. P. (2012). Soil organic matter  
816 turnover is governed by accessibility not recalcitrance. *Global Change Biology*, 18(6), 1781-  
817 1796.
- 818 Duveiller, G., Defourny, P., Desclee, B. and Mayaux, P. (2008), Deforestation in central Africa:  
819 estimates at regional, national and landscape levels by advanced processing of systematically-  
820 distributed Landsat extracts. *Remote Sensing of Environment*, 112, 1969- 1981.
- 821 Eisma, D. and Van Bennekom, A.J. (1978). The Zaire river and estuary and the Zaire outflow in

- 822 the Atlantic Ocean. *Netherlands Journal of Sea Research*, 12, 255–272.
- 823 Empresa de Pesquisa Energética (2013). Plano Decenal de Expansão de Energia 2022. Ministério  
824 de Minas e Energia. Brasília: Ministério de Minas e Energia.
- 825 Farella, N., Lucotte, M., Louchouart, P., and Roulet, M. (2001). Deforestation modifying  
826 terrestrial organic transport in the Rio Tapajos, Brazilian Amazon. *Organic Geochemistry*,  
827 32(12), 1443–1458.
- 828 Fearnside, P.M. (2002). Greenhouse gas emissions from a hydroelectric reservoir (Brazil's Tucuruí  
829 Dam) and the energy policy implications. *Water, Air, and Soil Pollution*, 133(1-4), pp.69-96.
- 830 Filizola, N., and Guyot, J.L. (2009), Suspended sediment yield in the Amazon basin. An  
831 assessment using the Brazilian national data set. *Hydrological Processes*, 23, 3207 – 3215.
- 832 Forsberg, B.R., Araujo-Lima, C.A.R.M., Martinelli, L.A., Victoria, R.L., Bonassi, J.A. (1993).  
833 Autotrophic carbon source for fish of the central Amazon. *Ecology*, 73, 643-652.
- 834 Fricke, A.T., Nittrouer, C.A., Ogston, A.S., Nowacki, D.J., Asp, N.E., Souza Filho, P.W., da Silva,  
835 M.S. and Jalowska, A.M. (2017). River tributaries as sediment sinks: Processes operating where  
836 the Tapajós and Xingu rivers meet the Amazon tidal river. *Sedimentology*, 64(6), pp.1731-1753.
- 837 Gagne-Maynard, W.C., Ward, N.D., Keil, R.G., Sawakuchi, H.O., Da Cunha, A.C., Neu, V., Brito,  
838 D.C., Da Silva Less, D.F., Diniz, J.E., De Matos Valerio, A. and Kampel, M. (2017). Evaluation  
839 of primary production in the Lower Amazon River based on a dissolved oxygen stable isotopic  
840 mass balance. *Frontiers in Marine Science*, 4, p.26.
- 841 Gerland, P., Raftery, A. E., Ševčíková, H., Li, N., Gu, D., Spoorenberg, T., et al. (2014). World  
842 population stabilization unlikely this century. *Science*, 346(6206), 234–237.
- 843 Hastie, A., Lauerwald, R., Ciais, P., and Regnier, P. (2019). Aquatic carbon fluxes dampen the  
844 overall variation of net ecosystem productivity in the Amazon basin: An analysis of the

- 845 interannual variability in the boundless carbon cycle. *Global Change Biology*, 25(6), 2094-  
846 2111.
- 847 Hastie, A., Lauerwald, R., Ciais, P., Papa, F., and Regnier, P. (2020). Historical and future  
848 contributions of inland waters to the Congo basin carbon balance. *Earth System Dynamics  
849 Discussions*, 1-49.
- 850 Hedges, J. I., Ertel, J. R., Quay, P. D., Grootes, P. M., Richey, J. E., Devol, A. H., et al. (1986a).  
851 Organic carbon-14 in the Amazon river system. *Science*, 231(4742), 1129–1131.
- 852 Hedges, J.I., Clark, W.A., Quay, P.D., Richey, J.E., Devol, A.H., and Santos, U.D.M. (1986b).  
853 Compositions and fluxes of particulate organic material in the Amazon River. *Limnology and  
854 Oceanography*, 31, 717- 738.
- 855 Hedges, J.I., Cowie, G.L., Richey, J.E., Quay, P.D., Benner, R., Strom, M., and Forsberg, B.R.  
856 (1994), Origins and processing of organic matter in the Amazon River as indicated by  
857 carbohydrates and amino acids. *Limnology and Oceanography*, 39, 743-761.
- 858 Hedges, J. I., and Keil, R.G. (1995), Sedimentary organic matter preservation: an assessment and  
859 speculative synthesis. *Marine Chemistry*, 49, 81-115.
- 860 Hedges, J. I., Keil, R.G., and Benner, R. (1997), What happens to terrestrial organic matter in  
861 the ocean? *Organic Geochemistry*, 27, 195-212.
- 862 Hedges, J.I., Mayorga, E., Tsamakis, E., McClain, M.E., Aufdenkampe, A.K., Quay, P.D., Richey,  
863 J.E., Benner, R., Opsahl, S., Black, B., Pimental, T., Quintanilla, J. and Maurice, L. (2000).  
864 Organic matter in Bolivian tributaries of the Amazon River: A comparison to the lower  
865 mainstream. *Limnology and Oceanography* 45, 1449-1466.
- 866 van Hees, P. A. W., Jones, D. L., Finlay, R., Godbold, D. L., and Lundström, U. S. (2005). The  
867 carbon we do not see—the impact of low molecular weight compounds on carbon dynamics

- 868 and respiration in forest soils: a review. *Soil Biology and Biochemistry*, 37(1), 1–13.
- 869 Hernes, P.J., and Benner, R. (2006), Terrigenous organic matter sources and reactivity in the North  
870 Atlantic Ocean and a comparison to the Arctic and Pacific oceans. *Marine Chemistry* 100, 66-  
871 79.
- 872 Hubau, W., Lewis, S.L., Phillips, O.L. *et al.* (2020). Asynchronous carbon sink saturation in  
873 African and Amazonian tropical forests. *Nature* 579, 80–87 [https://doi.org/10.1038/s41586-](https://doi.org/10.1038/s41586-020-2035-0)  
874 020-2035-0
- 875 Ibánhez, J. S. P., Diverrès, D., Araujo, M., and Lefèvre, N. (2015). Seasonal and interannual  
876 variability of sea-air CO<sub>2</sub> fluxes in the tropical Atlantic affected by the Amazon River plume.  
877 *Global Biogeochemical Cycles*, 29(10), 1640-1655.
- 878 Johnson, M. S., Lehmann, J., Riha, S. J., Krusche, A. V., Richey, J. E., Ometto, J. P. H., and Couto,  
879 E. G. (2008). CO<sub>2</sub> efflux from Amazonian headwater streams represents a significant fate for  
880 deep soil respiration. *Geophysical Research Letters*, 35(17).
- 881 Junk, W. J. and C. Howard-Williams, C. (1984). Ecology of aquatic macrophytes in Amazonia.  
882 In: Sioli, H. (ed.), *The Amazon: limnology and landscape ecology of a mighty tropical river*  
883 and its basin. Dr W. Junk Publishers, Dordrecht: 269–293.
- 884 Kaiser, K., and Kalbitz, K. (2012). Cycling downwards--dissolved organic matter in soils. *Soil*  
885 *Biology and Biochemistry*, 52, 29–32.
- 886 Kalbitz, K., Schwesig, D., Schmerwitz, J., Kaiser, K., Haumaier, L., Glaser, B., et al. (2003).  
887 Changes in properties of soil-derived dissolved organic matter induced by biodegradation. *Soil*  
888 *Biology and Biochemistry*, 35(8), 1129–1142.
- 889 Kellerman, A. M., Guillemette, F., Podgorski, D. C., Aiken, G. R., Butler, K. D., and Spencer, R.  
890 G. M. (2018). Unifying Concepts Linking Dissolved Organic Matter Composition to

- 891 Persistence in Aquatic Ecosystems. *Environmental Science and Technology*, 52(5), 2538–2548.
- 892 Laporte, N., Stabach, J.A., Grosch, R., Lin, T.S., and Goetz, S.J. (2007), Expansion of industrial  
893 logging in Central Africa. *Science* 316, 1451.
- 894 Laraque, A., Bricquet, J.P., Pandi, A., and Olivry, J.C. (2009), A review of material transport by  
895 the Congo River and its tributaries. *Hydrological Processes* 23, 3216-3224.
- 896 Lovett, G.M., Cole, J.J., Pace, M.L. (2006). Is Net Ecosystem Production Equal to Ecosystem  
897 Carbon Accumulation? *Ecosystems* Volume 9, Number 1, 152-155, DOI: 10.1007/s10021-005-  
898 0036-3
- 899 Lützow, M. V., Kögel-Knabner, I., Ekschmitt, K., Matzner, E., Guggenberger, G., Marschner, B.,  
900 and Flessa, H. (2006). Stabilization of organic matter in temperate soils: mechanisms and their  
901 relevance under different soil conditions—a review. *European Journal of Soil Science*, 57(4),  
902 426-445.
- 903 MacIntyre, S., Amaral, J.H.F., Barbosa, P.M., Cortés, A., Forsberg, B.R., and Melack, J.M.  
904 (2019). Turbulence and gas transfer velocities in sheltered flooded forests of the Amazon  
905 basin. *Geophysical Research Letters*. doi.org/10.1029/2019GL083948
- 906 Malhi, Y., and Grace, J. (2000). Tropical forests and atmospheric carbon dioxide. *Trends in*  
907 *Ecology and Evolution*, 15(8), 332-337.
- 908 Mann, P.J., Eglinton, T.I., McIntyre, C.P., Zimov, N., Davydova, A., Vonk, J.E., Holmes, R.M., and  
909 Spencer, R.G.M. (2015), Utilization of ancient permafrost carbon in headwaters of Arctic  
910 fluvial networks. *Nature Communications*, 6, doi:10.1038/ncomms8856.
- 911 Marin-Spiotta, E., Gruley, K.E., Crawford, J., Atkinson, E.E., Miesel, J.R., Greene, S., Cardona-  
912 Correa, C., and Spencer, R.G.M. (2014), Paradigm shifts in soil organic matter research affect  
913 interpretations of aquatic carbon cycling: transcending disciplinary and ecosystem boundaries.

- 914 *Biogeochemistry*, 117, 279-297.
- 915 Marwick, T. R., Tamooch, F., Teodoru, C.R., Borges, A.V., Darchambeau, F., and Bouillon, S.  
916 (2015), The age of river-transported carbon: A global perspective, *Global Biogeochemical*  
917 *Cycles*, 29, 122–137, doi:10.1002/2014GB004911
- 918 Mayorga, E., Aufdenkampe, A. K., Masiello, C. A., Krusche, A. V., Hedges, J. I., Quay, P. D., et  
919 al. (2005). Young organic matter as a source of carbon dioxide outgassing from Amazonian  
920 rivers. *Nature*, 436(7050), 538–541.
- 921 Meade, R. H., Dunne, T., Richey, J.E., Santos, U.M.m and Salati, E. (1985), Storage and  
922 remobilization of sediment in the lower Amazon River of Brazil, *Science*, 228, 488–490.
- 923 Medeiros, P.M., Seidel, M., Ward, N.D., Carpenter, E.J., Gomes, H.R., Niggemann, J., Krusche,  
924 A.V., Richey, J.E., Yager, P.L., Dittmar, T. (2015) Fate of the Amazon River dissolved organic  
925 matter in the tropical Atlantic Ocean. *Global Biogeochemical Cycles*, 29, 677-690.
- 926 Melack, J.M, and Forsberg, B. (2001) Biogeochemistry of Amazon floodplain lakes and associated  
927 wetlands. In: McClain, M.E., Victoria R.L., and Richey J.E. (eds) Biogeochemistry of the  
928 Amazon Basin and its role in a changing world. Oxford University Press, Oxford, pp. 235–276
- 929 Melack, J.M., Hess, L.L, Gastil, M, Forsberg, B.R., Hamilton, S.K., Lima, I.B.T., Novo, E.M.L.M.  
930 (2004). Regionalization of methane emissions in the Amazon basin with microwave remote  
931 sensing. *Global Change Biology* 10:530–544.
- 932 Melack, J. M., Hess, L. L., Gastil, M., Forsberg, B. R., Hamilton, S. K., Lima, I. B., and Novo, E.  
933 M. (2004). Regionalization of methane emissions in the Amazon Basin with microwave remote  
934 sensing. *Global Change Biology*, 10(5), 530-544.
- 935 Melack, J.M., and Engle, D (2009). An organic carbon budget for an Amazon floodplain lake.  
936 *Verhandlungen des Internationalen Verein Limnologie* 30:1179–1182

- 937 Melack, J.M. (2016). Aquatic Ecosystems. In L. Nagy et al. (eds.), *Interactions Between*  
938 *Biosphere, Atmosphere and Human Land Use in the Amazon Basin*, Ecological Studies 227,  
939 Springer-Verlag Berlin Heidelberg DOI 10.1007/978-3-662-49902-3\_7
- 940 Meybeck M. (2002), Riverine quality at the Anthropocene: Propositions for global space and time  
941 analysis, illustrated by the Seine River, *Aquatic Sciences*, 64, 376-393.
- 942 Mollenhauer, G., Schneider, R.S., Jennerjahn, T.C., Muller, P.J., and Wefer, G. (2004), Organic  
943 carbon accumulation in the South Atlantic Ocean: Its modern, mid- Holocene and last glacial  
944 distribution. *Global and Planetary Change*, 40, 249-266.
- 945 Moore, S., Evans, C. D., Page, S. E., Garnett, M. H., Jones, T. G., Freeman, C., et al. (2013). Deep  
946 instability of deforested tropical peatlands revealed by fluvial organic carbon fluxes. *Nature*,  
947 493(7434), 660-663.
- 948 Moreira-Turcq, P., Seyler, P., Guyot, J.L., Etcheber, H., (2003). Exportation of organic carbon  
949 from the Amazon river and its main tributaries. *Hydrological Processes*, 17, 1329–1344.
- 950 Onstad, G.D., Canfield, D.E., Quay, P.D., Hedges, J.I. (2000), Sources of particulate organic  
951 matter in rivers from the continental USA: Lignin phenol and stable carbon isotope  
952 composition. *Geochimica et Cosmochimica Acta*, 64, 3539-3546.
- 953 Opsahl, S., and Benner, R. (1997), Distribution and cycling of terrigenous dissolved organic matter  
954 in the ocean. *Nature*, 386, 480-482.
- 955 Pak, H., Zaneveld, J.R.V., and Spinrad, R.W. 1984. Vertical distribution of suspended particulate  
956 matter in the Zaire river, estuary and plume. *Netherlands Journal of Sea Research*, 17, 412–  
957 425.
- 958 Pangala, S., Enrich-Prast, A., Basso, L. et al. (2017). Large emissions from floodplain trees close  
959 the Amazon methane budget. *Nature* 552, 230–234 <https://doi.org/10.1038/nature24639>

- 960 Rabouille, C., Caprais, J.C., Lansard, B., Crassous, P., Dedieu, K., Reyss, J.-L., and Khripounoff,  
961 A. (2009), In situ measurements of sediment oxygen consumption and organic matter budget  
962 in the Southeast Atlantic continental margin close to the Congo Canyon. *Deep-Sea Research*,  
963 II, 56, 2223–2238.
- 964 Raymond, P.A., and Bauer, J.E. (2001), Riverine export of aged terrestrial organic matter to the  
965 North Atlantic Ocean. *Nature*, 409, 497-500.
- 966 Raymond, P. A., McClelland, J. W. , Holmes, R. M., Zhulidov, A. V., Mull, K., Peterson, B. J.,  
967 Striegl, R. G., Aiken, G. R., and Gurtovaya, T. Y. (2007), Flux and age of dissolved organic  
968 carbon exported to the Arctic Ocean: A carbon isotopic study of the five largest rivers. *Global*  
969 *Biogeochemical Cycles*, 21, GB4011, doi:10.1029/2007GB002934.
- 970 Raymond, P.A., Hartmann, J., Lauerwald, R., Sobek, S., McDonald, C., Hoover, M., et al.  
971 (2013). Global carbon dioxide emissions from inland waters. *Nature* 503, 355–  
972 359. doi:10.1038/nature12760
- 973 Raymond, P.A., and Spencer, R.G.M. (2015), Riverine DOM. In Hansell, D.A. and C.A. Carlson  
974 (eds) *Biogeochemistry of Marine Dissolved Organic Matter* (2<sup>nd</sup> Edition), AP, pp. 509-535.
- 975 Raymond, P. A., Saiers, J. E., and Sobczak, W. V. (2016). Hydrological and biogeochemical  
976 controls on watershed dissolved organic matter transport: Pulse-shunt concept. *Ecology*, 97(1),  
977 5-16.
- 978 Remington, S., Krusche, A., and Richey, J. (2011). Effects of DOM photochemistry on bacterial  
979 metabolism and CO<sub>2</sub> evasion during falling water in a humic and a whitewater river in the  
980 Brazilian Amazon. *Biogeochemistry*, 105(1-3), 185-200.
- 981 Richey, J. E., Meade, R.H., Salati, E., Devol, A.H., Nordin, C.F., and dos Santos, U. (1986),  
982 Water discharge and suspended sediment concentrations in the Amazon River: 1982–1984,

- 983 *Water Resources Research*, 22, 756–764.
- 984 Richey, J. E., Nobre, C., and Deser, C. (1989). Amazon River discharge and climate variability:  
985 1903 to 1985. *Science*, 246 (4926), 101-103. Richey, J. E., Hedges, J. I., Devol, A. H., Quay,  
986 P. D., Victoria, R., Martinelli, L., and Forsberg, B. R. (1990). Biogeochemistry of carbon in the  
987 Amazon River. *Limnology and Oceanography*, 35(2), 352–371.
- 988 Richey, J. E., J. I. Hedges, A. H. Devol, P. D. Quay, R. Victoria, L. Martinelli, and B. R. Forsberg.  
989 (1990). Biogeochemistry of carbon in the Amazon River. *Limnology and Oceanography*, 35:  
990 352-371.
- 991 Richey, J.E., Melack, J.M., Aufdenkampe, A.K., Ballester, V.M., and Hess, L.L. (2002). Carbon  
992 dioxide evasion from central Amazonian wetlands as a significant source of atmospheric CO<sub>2</sub>  
993 in the tropics. *Nature* 416,617–620. doi:10.1038/416617a
- 994 Rocher-Ros, G., Sponseller, R. A., Lidberg, W., Mörth, C. M., and Giesler, R. (2019). Landscape  
995 process domains drive patterns of CO<sub>2</sub> evasion from river networks. *Limnology and*  
996 *Oceanography Letters*, 4(4), 87-95.
- 997 Saliot, A., Mejanelle, L., Scribe, P., Fillaux, J., Pepe, C., Jabaud, A., and Dagaut, J. (2001).  
998 Particulate organic carbon, sterols, fatty acids and pigments in the Amazon River system.  
999 *Biogeochemistry* 53:79–103.
- 1000 Savoye, B., Babonneau, N., Dennielou, B. and Bez, M. (2009). Geological overview of the  
1001 Angola- Congo margin, the Congo deep-sea fan and its submarine valleys. *Deep Sea Research*  
1002 *Part II*, 56, 2169-2182.
- 1003 Sawakuchi, H.O., Bastviken, D., Sawakuchi, A.O., Krusche, A.V., Ballester, M.V. and Richey,  
1004 J.E. (2014). Methane emissions from Amazonian Rivers and their contribution to the global  
1005 methane budget. *Global Change Biology*, 20(9), pp.2829-2840.

- 1006 Sawakuchi, H.O., Bastviken, D., Sawakuchi, A.O., Ward, N.D., Borges, C., Tsai, S.M., Richey,  
1007 J.E., Ballester, M.V.R., Krusche, A.V. (2016). Oxidative mitigation of methane evasion in large  
1008 Amazonian rivers. *Global Change Biology*. 22 (3), 1075-1085.
- 1009 Sawakuchi, H.O., Neu, V., Ward, N.D., Barros, M.D.L.C., Valerio, A.M., Gagne-Maynard, W.,  
1010 Cunha, A.C., Less, D.F., Diniz, J.E., Brito, D.C. and Krusche, A.V. (2017). Carbon dioxide  
1011 emissions along the lower Amazon River. *Frontiers in Marine Science*, 4, p.76.
- 1012 Schefuß, E., Eglinton, T.I., Spencer-Jones, C.L., Rullkötter, J., De Pol-Holz, R., Talbot, H.M.,  
1013 Grootes, P.M. and Schneider, R.R., (2016). Hydrologic control of carbon cycling and aged  
1014 carbon discharge in the Congo River basin. *Nature Geoscience*, 9(9), 687-690.
- 1015 Seidel, M., Yager, P.L., Ward, N.D., Carpenter, E.J., Gomes, H.R., Krusche, A.V., Richey, J.E.,  
1016 Dittmar, T. and Medeiros, P.M. (2015). Molecular-level changes of dissolved organic matter  
1017 along the Amazon River-to-ocean continuum. *Marine Chemistry*, 177, pp.218-231.
- 1018 Seidel, M., Dittmar, T., Ward, N.D., Krusche, A.V., Richey, J.E., Yager, P.L. and Medeiros, P.M.  
1019 (2016). Seasonal and spatial variability of dissolved organic matter composition in the lower  
1020 Amazon River. *Biogeochemistry*, 131(3), pp.281-302.
- 1021 Sioli, H. (ed). 1984. The Amazon. Springer Netherlands. DOI10.1007/978-94-009-6542-3. 800p.
- 1022 Soto, D.X., Decru, E., Snoeks, J., Verheyen, E., de Walle, L.V., Bamps, J., Mambo, T., and  
1023 Bouillon, S. (2019). Terrestrial contributions to Afrotropical aquatic food webs: The Congo  
1024 River case. *Ecology and Evolution*, 9, 10746-10757.
- 1025 Spencer, R.G.M., Stubbins, A., Hernes, P.J., Baker, A., Mopper, K., Aufdenkampe, A.K., Dyda,  
1026 R.Y., Mwamba, V.L., Mangangu, A.M., Wabakanghanzi, J.N., and Six, J. (2009).  
1027 Photochemical degradation of dissolved organic matter and dissolved lignin phenols from the  
1028 Congo River. *Journal of Geophysical Research: Biogeosciences*. 114, G03010, doi:

- 1029 10.1029/2009JG000968.
- 1030 Spencer, R. G. M., Hernes, P. J., Aufdenkampe, A. K., Baker, A., Gulliver, P., Stubbins, A., et al.  
1031 (2012). An initial investigation into the organic matter biogeochemistry of the Congo River.  
1032 *Geochimica et Cosmochimica Acta*, 84, 614–627.
- 1033 Spencer, R. G. M., Mann, P. J., Dittmar, T., Eglinton, T. I., McIntyre, C., Holmes, R. M., et al.  
1034 (2015). Detecting the signature of permafrost thaw in Arctic rivers. *Geophysical Research*  
1035 *Letters*, 42(8), 2015GL063498.
- 1036 Spencer, R.G.M., Hernes, P.J., Dinga, B., Wabakanghanzi, J.N., Drake, T.W., and Six, J. (2016).  
1037 Origins, seasonality and fluxes of organic matter in the Congo River. *Global Biogeochemical*  
1038 *Cycles*, 30 (7), 1105-1121.
- 1039 Spencer, R. G. M., Kellerman, A. M., Podgorski, D. C., Macedo, M. N., Jankowski, K., Nunes,  
1040 D., and Neill, C. (2019). Identifying the Molecular Signatures of Agricultural Expansion in  
1041 Amazonian Headwater Streams. *Journal of Geophysical Research: Biogeosciences*, 124(6),  
1042 1637–1650.
- 1043 St. Louis, V.L., Kelly, C.A., Duchemin, É., Rudd, J.W. and Rosenberg, D.M., 2000. Reservoir  
1044 surfaces as sources of greenhouse gases to the atmosphere: A global estimate. *BioScience*,  
1045 50(9), pp.766-775.
- 1046 Stubbins, A., Spencer, R. G., Chen, H., Hatcher, P. G., Mopper, K., Hernes, P. J., Mwamba, V.L.,  
1047 Mangangu, A.M., Wabakanghanzi, J.N., and Six, J. (2010). Illuminated darkness: Molecular  
1048 signatures of Congo River dissolved organic matter and its photochemical alteration as revealed  
1049 by ultrahigh precision mass spectrometry. *Limnology and Oceanography*, 55(4), 1467-1477.
- 1050 Thomas, S. M., Neill, C., Deegan, L. A., Krusche, A. V., Ballester, V. M., and Victoria, R. L.  
1051 (2004). Influences of land use and stream size on particulate and dissolved materials in a small

- 1052 Amazonian stream network. *Biogeochemistry*, 68(2), 135–151.
- 1053 Trancoso, R. (2006). Land cover changes, and disturbances in hydrological response of  
1054 Amazonian watersheds, *Master's thesis*, Manaus: INPA.
- 1055 Tranvik, L. J., Downing, J. A., Cotner, J. B., Loiselle, S. A., Striegl, R. G., Ballatore, T. J., et al.  
1056 (2009). Lakes and reservoirs as regulators of carbon cycling and climate. *Limnology and*  
1057 *Oceanography*, 54(6part2), 2298-2314.
- 1058 Valerio, A.M., Kampel, M., Ward, N.D., Sawakuchi, H.O., Cunha, A.C., Krusche, A.V., Richey,  
1059 J.E. (in press) Seasonal and inter-annual variability of carbon dioxide fluxes in the Amazon  
1060 River plume based on Soil Moisture and Ocean Salinity satellite data. *Continental Shelf*  
1061 *Research*
- 1062 Vannote, R. L., Minshall, G.W., Cummins, K.W., Sedell, J.R., and Cushing, C.E. 1980. The river  
1063 continuum concept. *Canadian Journal of Fisheries and Aquatic Sciences*. 37: 130-137.
- 1064 Ward, N.D., Keil, R.G., Medeiros, P.M., Brito, D.C., Cunha, A.C., Dittmar, T., Yager, P.L.,  
1065 Krusche, A.V., Richey, J.E. (2013). Degradation of terrestrially derived macromolecules in the  
1066 Amazon River. *Nature Geoscience*, 6, 530-533.
- 1067 Ward, N.D., Krusche, A.V., Sawakuchi, H.O., Brito, D.C., Cunha, A.C., Moura, J.M.S., da Silva,  
1068 R., Yager, P.L., Keil, R.G. and Richey, J.E. (2015). The compositional evolution of dissolved  
1069 and particulate organic matter along the lower Amazon River—Óbidos to the ocean. *Marine*  
1070 *Chemistry*, 177, pp.244-256.
- 1071 Ward, N.D., Bianchi, T.S., Sawakuchi, H.O., Gagne-Maynard, W., Cunha, A.C., Brito, D.C., Neu,  
1072 V., de Matos Valerio, A., da Silva, R., Krusche, A.V. and Richey, J.E. (2016). The reactivity  
1073 of plant-derived organic matter and the potential importance of priming effects along the lower  
1074 Amazon River. *Journal of Geophysical Research: Biogeosciences*, 121(6), pp.1522- 1539.

- 1075 Ward, N.D., Bianchi, T.S., Medeiros, P.M., Seidel, M., Richey, J.E., Keil, R.G. and Sawakuchi,  
1076 H.O. (2017). Where carbon goes when water flows: carbon cycling across the aquatic  
1077 continuum. *Frontiers in Marine Science*, 4, p.7.
- 1078 Ward, N.D., Sawakuchi, H.O., Neu, V., Less, D.F., Valerio, A.M., Cunha, A.C., Kampel, M.,  
1079 Bianchi, T.S., Krusche, A.V., Richey, J.E. and Keil, R.G. (2018a). Velocity-amplified  
1080 microbial respiration rates in the lower Amazon River. *Limnology and Oceanography Letters*,  
1081 3(3), pp.265-274.
- 1082 Ward, N.D., Sawakuchi, H.O., Richey, J.E. (2018b) The Amazon River's ecosystem—where land  
1083 meets the sea. *Eos*. 99. <https://doi.org/10.1029/2018EO088573>
- 1084 Ward, N.D., Sawakuchi, H.O., Richey, J.E., Keil, R.G., and Bianchi, T.S. (2019). Enhanced  
1085 aquatic respiration rates associated with mixing of clearwater tributary and turbid Amazon  
1086 River waters. *Frontiers Earth Science Section Marine Biogeochemistry*. DOI:  
1087 10.3389/feart.2019.00101
- 1088 Ward, N. D., Megonigal, J. P., Bond-Lamberty, B., Bailey, V. L., Butman, D., Canuel, E. A., et  
1089 al. (2020). Representing the function and sensitivity of coastal interfaces in Earth system  
1090 models. *Nature Communications*, 11(1), 1-14.
- 1091 Williams, P. M., and Druffel, E. R. (1987). Radiocarbon in dissolved organic matter in the central  
1092 North Pacific Ocean. *Nature*, 330(6145), 246-248.
- 1093 Williams, M. R., and Melack, J. M. (1997). Solute export from forested and partially deforested  
1094 catchments in the central Amazon. *Biogeochemistry*, 38(1), 67–102.
- 1095 Winemiller, K.O., McIntyre, P.B., Castello, L., et al. (2016), Balancing hydropower and  
1096 biodiversity in the Amazon, Congo and Mekong. *Science*, 351, 128-129
- 1097 Wissmar, R. C., Richey, J.E., Stallard, R.F., and Edmond, J.M. (1981). Plankton metabolism and

1098 carbon processes in the Amazon River, its tributaries, and floodplain waters, Peru-Brazil, May-  
1099 June 1977. *Ecology*, 62: 1622-1633.

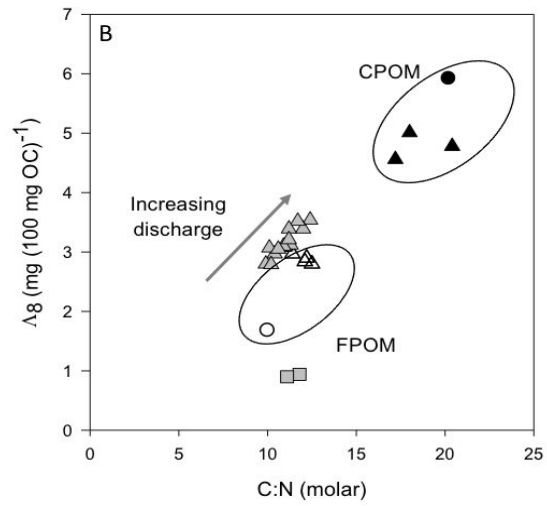
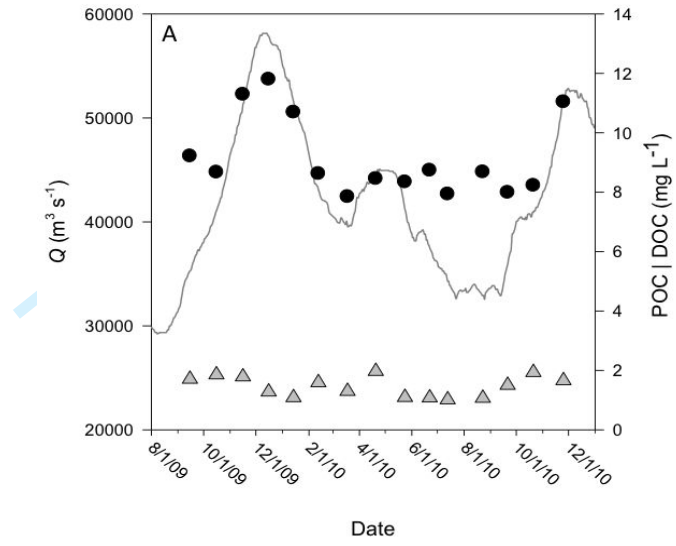
1100 Zarfl, C., Lumsdon, A.E., Berlekamp, J., Tydecks, L. and Tockner, K. (2015). A global boom in  
1101 hydropower dam construction, *Aquatic Sciences* 77:161– 170.

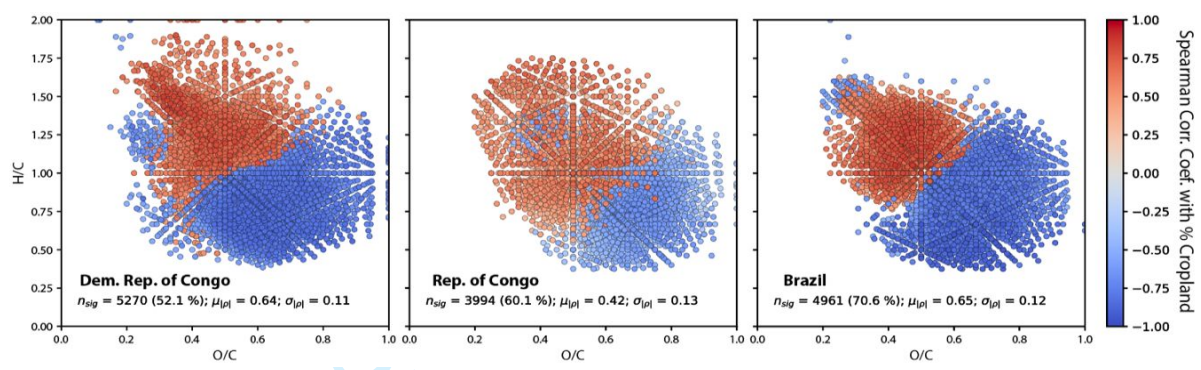
1102 **Acknowledgments**

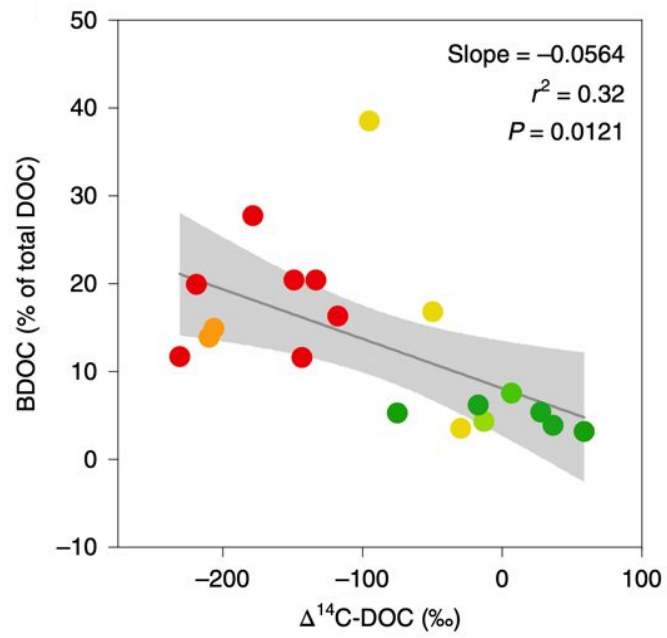
This work was partially supported by funding provided by the São Paulo Research Foundation (FAPESP 2018/18491-4), US National Science Foundation DEB- 1754317 and OCE 1464396 and DMR-1157490 and DMR-1644779 to the National High Magnetic Field Laboratory.

For Review Only









View Only